ASYMPTOTIC PERFORMANCE ANALYSIS FOR EGC AND SC OVER ARBITRARILY CORRELATED NAKAGAMI-*m* FADING CHANNELS

by

XIANCHANG LI

B.Eng., Northwestern Polytechnical University, China, 2004

A THESIS SUBMITTED IN PARTIAL FULFILLMENT OF
THE REQUIREMENTS FOR THE DEGREE OF

MASTER OF APPLIED SCIENCE

in

The College of Graduate Studies

(Electrical Engineering)

THE UNIVERSITY OF BRITISH COLUMBIA

(OKANAGAN)

April 2011

Abstract

The multi-branch diversity combining technique has been widely used in wireless communications systems to overcome the adverse effect of multipath fading. The three most popular diversity combining schemes are selection combining (SC), equal gain combining (EGC), and maximal ratio combining (MRC). In the performance analysis of multi-branch diversity combining, the asymptotic technique is an attractive approach to obtain compact and accurate error rate and outage probability in large signal-to-noise ratio (SNR) regions. Asymptotic performance can be obtained either in the time domain by finding the probability density function (PDF) of the instantaneous output SNR, or in the frequency domain by finding the moment generating function (MGF) of the square root of the instantaneous output SNR. In this thesis, the PDF of the instantaneous SNR at the output of selection combiner and the MGF of the square root of the instantaneous SNR at the output of equal gain combiner over arbitrarily correlated Nakagami-m fading channels are derived and used to obtain asymptotic error rate and outage probability expressions of SC and EGC, respectively. These expressions provide accurate and rapid estimation of error rates and outage probabilities. The accuracy of our analytical results is verified by computer simulation. More importantly, our analytical results provide physical insights into the transmission behavior of EGC and SC over arbitrarily correlated Nakagami-m fading channels. For instance, it is shown that the asymptotic error rates over correlated branches can be obtained by scaling the asymptotic error rates over independent branches with a factor, $\det^m(\mathbf{M})$, where $\det(\mathbf{M})$ is the determinant of matrix $\mathbf{M}$ whose elements are the square root of corresponding elements in the branch power covariance correlation matrix $\mathbf{R}$. A similar relationship can also be found for the outage probabilities.

Table of Contents

Appendices

List of Tables

List of Figures

List of Acronyms

Acronyms	Definitions
AWGN	Additive White Gaussian Noise
BER	Bit Error Rate
BDPSK	Binary Differential Phase Shift Keying
BNCFSK	Binary Noncoherent Frequency Shift Keying
BPSK	Binary Phase Shift Keying
CDF	Cumulative Distribution Function
EGC	Equal Gain Combining
LOS	Line-of-Sight
MGF	Moment Generating Function
M-PAM	M-ary Pulse Amplitude Modulation
M-PSK	M-ary Pulse Shift Keying
M-QAM	M-ary Quadrature Amplitude Modulation
MRC	Maximal Ratio Combining
PDF	Probability Density Function
PSD	Power Spectral Density
RV	Random Variable
SC	Selection Combining
SER	Symbol Error Rate
SNR	Signal-to-Noise Ratio

List of Symbols

Symbols	Definitions
$[\cdot]^T$	Matrix transpose operator
d	Transmitted data symbol
$\det(\mathbf{M})$	Determinant of matrix $\mathbf{M}$
$\exp(\cdot)$	Exponential function
$\mathrm{E}[\cdot]$	The expectation of a RV
E_S	Average symbol energy of the transmitted data symbol
$f(\beta)$	PDF of RV β
$f(\gamma)$	PDF of instantaneous SNR
$f(x)$	PDF of RV X
$f_{\gamma_{SC}}(\gamma)$	PDF of γ_{SC}
$f(r_1, r_2, \cdots, r_L)$	Joint PDF of $R_1, R_2, \cdots, R_L$
$F(a,b;c;z)$	Hypergeometric function defined as $F(a,b;c;z) = \frac{\Gamma(c)}{\Gamma(a)\Gamma(b)} \sum_{n=0}^{\infty} \frac{\Gamma(a+n)\Gamma(b+n)}{\Gamma(c+n)} \frac{z^n}{n!}$
$F(r\|z)$	Marginal CDF of R depending on Z
$F(r_1, r_2, \cdots, r_L\|z)$	Conditional CDF of $R_1, R_2, \cdots, R_L$ depending on Z
$F(r_1, r_2, \cdots, r_L)$	Joint CDF of $R_1, R_2, \cdots, R_L$
$F_{\gamma_{SC}}(\gamma)$	CDF of γ_{SC}
G_c	Coding gain
G_d	Diversity gain
G_{il}	Zero-mean complex Gaussian RV

h_i	Channel fading amplitude in the i-th branch
H_i	Nakagami-m RV
$I_v(\cdot)$	vth-order modified Bessel function of the first kind defined as $I_v(x) = \sum_{k=0}^{\infty} \frac{(x/2)^{v+2k}}{k!\Gamma(v+k+1)}$
$\mathscr{M}_h(s)$	MGF of RV h
$\max\{\gamma_i\}_{i=1}^{L}$	Maximum of $\gamma_1, \gamma_2, \cdots, \gamma_L$
n_i	Complex AWGN in the i-th branch
N_0	Power spectral density of complex AWGN
$o()$	Small o notation
p	Parameter in the conditional SER
$p_e(\beta)$	Conditional SER in terms of β
$p_e(\gamma)$	Conditional SER in terms of γ
P_e	Average SER for coherent or noncoherent modulation
P_e^E	Asymptotic SER of EGC reception with coherent modulation
$P_e^{S,C}$	Asymptotic SER of SC reception with coherent modulation
$P_e^{S,N}$	Asymptotic SER of SC reception with noncoherent modulation
$(P_e^{EGC})_{asym}$	Asymptotic SER of EGC over arbitrarily correlated Nakagami-m fading channels
$(P_{e,i}^{EGC})_{asym}$	Asymptotic SER of EGC over independent Nakagami-m fading channels
$(P_e^{SC})_{asym}$	Asymptotic SER of SC over arbitrarily correlated Nakagami-m fading channels
$(P_{e,i}^{SC})_{asym}$	Asymptotic SER of SC over independent Nakagami-m fading channels
$P_{out}^E(\gamma_{th})$	Asymptotic outage probability of EGC reception
$P_{out}^S(\gamma_{th})$	Asymptotic outage probability of SC reception
q	Parameter in the conditional SER

$Q(\cdot)$	Gaussian Q-function defined as $Q(x) = \int_x^\infty \frac{1}{\sqrt{2\pi}} \exp\left(-y^2/2\right) dy$
$Q_v(\alpha, \beta)$	Generalized Marcum Q-function defined as $Q_v(\alpha, \beta) = \int_\beta^\infty x \left(\frac{x}{\alpha}\right)^{v-1} e^{-\frac{x^2+\alpha^2}{2}} I_{v-1}(\alpha x)\, dx$
r_i	Received signal in the i-th branch
r_{EGC}	Output signal of equal gain combiner
r_{MRC}	Output signal of maximal ratio combiner
$\mathbf{S}^{-1}$	Inverse of matrix $\mathbf{S}$
$\mathrm{Var}[\cdot]$	Variance of a RV
w_i	Weighting factor in the i-th branch
β	A RV depending on the channel statistics
γ	Instantaneous SNR at the output of the diversity combiner
γ_{EGC}	Instantaneous SNR at the output of equal gain combiner
γ_{MRC}	Instantaneous SNR at the output of maximal ratio combiner
γ_{SC}	Instantaneous SNR at the output of selection combiner
γ_i	Instantaneous SNR of the i-th branch
$\bar{\gamma}$	The average SNR at the combiner output
Γ_i	Average SNR of the i-th branch
$\Gamma(\cdot)$	Gamma function defined as $\Gamma(x) = \int_0^\infty t^{x-1} e^{-t} dt$
$\gamma(m, z)$	Incomplete Gamma function defined as $\gamma(m, z) = \int_0^z t^{m-1} e^{-t} dt$
$\delta_{u,v}$	Kronecker delta function
ρ_i	Correlation factor
φ_i	Channel fading phase in the i-th branch
$\mathcal{N}\left(\mu, \sigma^2\right)$	Gaussian distributed with mean μ and variance σ^2
$\chi_n\left(0, \sigma_i^2\right)$	Central chi-square distribution with n degrees of freedom and common Gaussian variance σ_i^2

$\chi_n\left(s, \sigma_i^2\right)$	Noncentral chi-square distribution with n degrees of freedom, noncentrality parameter s^2 and common Gaussian variance σ_i^2

Acknowledgments

I am deeply grateful to my supervisor Dr. Julian Cheng for his enthusiasm, guidance, advice, encouragement, and support. I will continue to be influenced by his rigorous scholarship, clarity in thinking, and professional integrity.

I would like to express my thanks to Dr. Heinz Bauschke for his willingness to serve as my external examiner. I would also like to thank Dr. Richard Klukas and Dr. Jonathan Holzman for serving on the committee. I really appreciate their valuable time and constructive comments on my thesis.

I am also grateful to my dear colleagues Xian Jin, Maggie Luyan Mei, Mingbo Niu, Nathan Nianxin Tang, André Johnson, Vicki Feng Wei, Sapphire Yu Lan, Yeyuan Xiao, Yuefeng Yao, and Chiun-Shen Liao for sharing their academic experiences and constructive viewpoints generously with me during our discussions. Special thanks are given to Xuegui Song for his long-lasting help in research and daily life since 2003. I would also like to thank my dear friends Kefeng Xu, Xiaosa Zhang, Xiangkui Song, Er'tao Lv, Pengfei Zhou, and Shuaibin Li for their help.

Finally, I would like to thank my parents, sister, and brothers for their patience, understanding and support over all these years. I also want to thank my girlfriend and her parents for their encouragement and support. All my achievements would not have been possible without their constant encouragement and support.

Chapter 1

Introduction

1.1 Background and Motivation

In the 1860s, James Clerk Maxwell proposed Maxwell's equations, which form the foundation of electromagnetics and make wireless communications possible. However, it was not until 1895 that Guglielmo Marconi opened the way for modern wireless communications by transmitting the Morse code for the letter 'S' over a distance of approximately one and a half kilometers utilizing electromagnetic waves [1]. Since then, wireless communications have become a significant element of modern society. From satellite broadcasting to wireless Internet to the now ubiquitous cellular telephones, wireless communications have revolutionized the way societies function. On the one hand, wireless communications have gained wide popularity around the world. For instance, it is reported that the number of mobile phone subscribers is on the order of 4 billion currently and will rise to 5.6 billion in 2013 worldwide. On the other hand, wireless communications are faced with a number of challenges, among which multipath fading is the main cause leading to system degredation.

Multipath fading is mainly caused by the scattering, reflection, refraction, and diffraction of radiowaves when wireless signals go through complex physical mediums. Multipath fading leads to a loss of signal power without reducing noise power, and hence causing poor performance in wireless communication systems. The diversity concept was introduced to overcome the adverse effects of multipath fading on the performance of wireless communication systems by providing multiple faded replicas of the same signal at the receiver [2]. The intuition behind this concept is to exploit the low probability of concurrence of deep fades in all the replicas. In the spatial domain, diversity can be realized through multiple-receiver antennas, i.e., antenna diversity. Multi-branch diversity combining is an effective antenna diversity technique to combat the detrimental effects of multipath fading in wireless communications [3]. The three most popular diversity combining schemes are maximal ratio combining (MRC), selection combining (SC), and equal gain combining (EGC). Among them, MRC is the optimal diversity combiner but with high implementation complexity; SC and EGC provide comparable performance to MRC with relatively lower complexity.

In the study of diversity combining over correlated fading channels, analytical methods have been used to obtain accurate expressions for the average error rate and outage probability. While exact, the results are often complicated and difficult to apply since they generally demand one or two fold numerical integration and the exactness for the estimation of the average error rate and outage probability may be constrained by a selected numerical integration routine. In addition, these analytical results usually cannot provide useful physical insights into the transmission characteristics of correlated fading channels [4]. However, the asymptotic technique is a powerful analytical tool that usually provides compact and accurate estimation for error rate and outage probability in large signal-to-noise ratio (SNR) regions.

Besides the lower computational complexity, another significant advantage of asymptotic analysis is that the resulting solutions can often reveal some important insights that can not be easily obtained otherwise. For instance, Liu *et al.* observed that the asymptotic error rates of MRC, EGC, and SC over arbitrarily correlated Rayleigh channels can be obtained by scaling the asymptotic error rates over independent branches with the determinant of the normalized channel correlation matrix [5].

1.2 Literature Review

In the study of multi-branch diversity combining, performance analyses over independent fading channels have been widely published (see references in [2]). However, correlated fading among several diversity branches exists for many real systems [6], [7] due to the insufficient separation between the antennas. Therefore, quantitative analysis of the degradation of diversity systems due to correlated fading is important from both theoretical and practical standpoints. While a comprehensive theoretical performance analysis for MRC over various correlated fading channels is available, it is challenging for SC and EGC reception. This is because, with the exception of the dual-branch case, the cumulative distribution function (CDF) or probability density function (PDF) at the output of SC and EGC combiners operating over correlated branches is generally unknown.

A number of researchers have studied the performance of SC and EGC over correlated fading channels. For SC, most of the existing performance analysis over correlated fading channels has primarily focused on two or three branches [8–12]. In [13], Zhang and Lu proposed a general approach for studying L-branch SC in arbitrarily correlated fading. However, their method requires an L-dimensional integration, and the computation complexity increases exponentially with L [14]. In [15], Karagiannidis *et al.* obtained an expression for the joint CDF of multivariate Nakagami-m random variables (RVs) with exponential correlation, and this result was subsequently applied to the performance analysis of SC over correlated Nakagami-m fading channels. In another related work, Karagiannidis *et al.* proposed an efficient approach for evaluating the PDF and CDF of multiple Nakagami-m RVs with arbitrary correlation by approximating the correlation matrix with a Green's matrix [16]. However, their results were expressed in terms of an infinite series whose convergence can be slow when L is large and when the correlation coefficient is close to one. Recently, Chen and Tellambura derived the CDF of L-branch SC output SNR in equally correlated Nakagami-m fading by noting that a set of equally correlated complex Gaussian RVs can be obtained by linearly combining a set of independent Gaussian RVs [17]. Their technique was further applied by Zhang and Beaulieu for the performance analysis of generalized SC in arbitrarily correlated Nakagami-m fading [14]. Analytical solutions presented in [14] and [17], while exact, are complex and can be difficult to apply because they require double integration involving the m-th order generalized Marcum Q-function.

The exact performance analysis of EGC over correlated fading channels with arbitrary diversity order is equally challenging. Chen and Tellambura studied the performance of EGC in equally correlated Nakagami-m fading channels in [18], where the equally correlated Nakagami-m fading channels are transformed into a set of conditionally independent chi-square RVs and the moments of the EGC output SNR are expressed in terms of the Appell hypergeometric function. This solution, while exact, is complex and can be difficult to apply because it requires multiple numerical integrations. Karagiannidis analyzed the performance of EGC by approximating the moment generating function (MGF) of the output SNR, where the moments are determined exactly only for exponentially correlated Nakagami-m channels in terms of a multi-fold infinite series [19]. More recently, various simple and accurate approximations to the PDF of the sum of an arbitrary number of correlated Nakagami-m RVs are proposed in [20–23], which then are used for analytical EGC performance evaluation. All of the approaches proposed in [19–23] are complex because they require approximations for the MGF of the output SNR or the PDF of a sum of arbitrary number of Nakagami-m RVs.

The asymptotic technique described in [24], [25] is a powerful analytical tool to obtain accurate error rate and outage probability in large SNR regions. Let $\gamma = \beta\bar{\gamma}$ be the instantaneous SNR at the output of the diversity combiner, where β is a RV depending on the channel statistics and $\bar{\gamma}$ is the average SNR at the combiner output. For coherent modulation, the conditional symbol error rate (SER) in terms of γ is $p_e(\gamma) = pQ\left(\sqrt{q\gamma}\right)$, where $Q(\cdot)$ is one-dimensional Gaussian Q-function defined as $Q(x) = \int_x^\infty \frac{1}{\sqrt{2\pi}} \exp\left(-y^2/2\right) dy$ [2, eq. (4.1)], and p and q are constants related to the modulation formats. In [25], Wang and Giannakis observed that the conditional SER curve for coherent modulation behaves like an impulse function when instantaneous SNR is close to zero and the conditional SER is nearly zero for large instantaneous SNR (see Fig. 1.1). For correlated fading channels, the expression of $f(\gamma)$ can be difficult to obtain. Since the average SER is defined as

$$P_e = \int_0^\infty p_e(\gamma) f(\gamma) d\gamma \tag{1.1}$$

where $f(\gamma)$ is the PDF of instantaneous SNR, based on the observation of Wang and Giannakis, one can approximate the unknown PDF of the instantaneous SNR near its origin to compute the average SER for large values of average SNR. The PDF near zero can be derived from a Taylor series expansion. Finally, one can obtain the asymptotic average SER by (1.1). This is the fundamental idea of asymptotic techniques for performance analysis over correlated fading channels. Another approach, which can also yield the same asymptotic solution, is to calculate the MGF of the instantaneous SNR [25]. The asymptotic technique is suitable for providing highly accurate estimation for error rate and outage probability in large SNR regions, and for revealing physical insights into the transmission characteristics of multi-branch diversity combining over correlated fading channels.

1.3 Thesis Outline

This thesis consists of five chapters. Chapter 1 presents background knowledge of wireless communication developments and technologies. In modern wireless communication, mitigating the detrimental effects of multipath fading is important for any mature wireless communication system. Multi-branch space diversity is commonly used to improve the error rate performance of wireless communication systems. However, the analytical expressions for the error rate of diversity combining systems are often complex and unfeasible for correlated diversity branches. This motivates researchers to apply asymptotic techniques to study the error rate and outage probability of diversity combining systems in large SNR regions.

Chapter 2 provides detailed technical background for the entire thesis. Firstly, multipath fading is presented and the three basic and most widely used fading models, namely Raleigh,

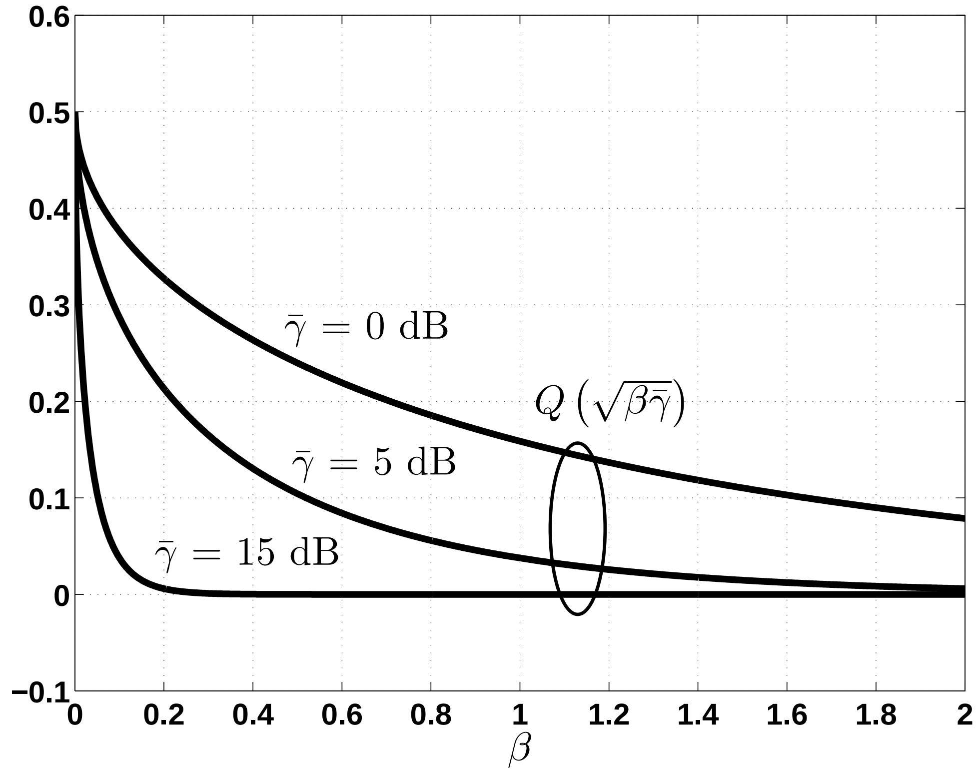

Figure 1.1: $Q\left(\sqrt{\beta\bar{\gamma}}\right)$ as functions of β for $\bar{\gamma} = 0$, 5, and 15 dB.

Rician and Nakagami-m fadings, are introduced. Secondly, the three most popular diversity schemes, namely MRC, EGC, and SC, are explained. Thirdly, the asymptotic technique is reviewed to show how the approximate MGFs or PDFs can be used to calculate the asymptotic error rate. Finally, a single integral representation is presented for the joint PDF of multiple correlated Nakagami-m RVs with specified correlation matrix.

In Chapter 3, we derive a new series representation of the generalized Marcum Q-function and give a simple accurate approximation for Marcum Q-function $Q_m(\alpha,\beta)$ when $\beta \to 0^+$. Utilizing this approximation, we obtain the PDF of the instantaneous SNR at the output of SC when SNR is near its origin and then derive closed form expressions for asymptotic SER and outage probability.

In Chapter 4, using the series expansion of the modified Bessel function of the first kind, we obtain the MGF of the square root of instantaneous SNR at the output of the equal gain combiner, and then derive the asymptotic average SER and outage probability of EGC over arbitrarily correlated Nakagami-m channels.

Chapter 5 summarizes the entire thesis and lists our contributions in this thesis. In addition, future work related to our current research is suggested.

Chapter 2

Multipath Fading and Diversity Combining Techniques

In this chapter, we will present some background knowledge concerning multipath fading, diversity combining techniques, the asymptotic technique, as well as construction of multiple Nakagami-m random variables with specified correlation matrix.

2.1 Multipath Fading

Radiowave propagation through wireless channels is a complicated process characterized by various effects such as multipath fading and shadowing. Multipath fading is due to the constructive and destructive combination of randomly delayed, reflected, scattered, and diffracted signal components. This type of fading is relatively fast and therefore is responsible for short-term signal variations, where both the signal envelope and signal phase fluctuate over time.

Depending on the relative relation between the symbol period of the transmitted signal and the coherence time of fading channels, fading can be classified into slow fading and fast fading [2], [3]. Coherence time is defined as the time period over which we can consider the fading process to be correlated. Slow fading occurs when the symbol duration is less than the channel coherence time, and fast fading is the opposite. Similarly, according to the relative relation between the transmitted signal bandwidth and the channel coherence bandwidth, fading can also be classified into frequency-nonselective fading and frequency-selective fading. Coherence bandwidth is defined as the frequency range over which the fading process is correlated. If the transmitted signal bandwidth is much smaller than the channel coherence bandwidth, the fading is considered to be flat, and otherwise it is frequency selective.

In this thesis, we only focus on slow and frequency-nonselective flat fading channels. When the multipath fading process possesses these properties, it is common to use statistical distributions to describe the random behavior of the received signal amplitude. Most widely used statistical models include the Rayleigh, Rician, and Nakagami-*m* distributions.

2.1.1 Rayleigh Distribution

The Rayleigh distribution is frequently used to model the time varying characteristics of the received signal amplitude in a wireless channel where there is no direct line-of-sight (LOS) path between the transmitter and the receiver. It is well known that the envelope of the sum of two independent and identically distributed (i.i.d.) Gaussian signals with zero mean and variance σ^2 obeys a Rayleigh distribution. The PDF of the Rayleigh distribution is given by

$$\begin{aligned} f(x) &= \frac{x}{\sigma^2} \exp\left(-\frac{x^2}{2\sigma^2}\right) \\ &= \frac{2x}{\Omega} \exp\left(-\frac{x^2}{\Omega}\right), \; x \geq 0 \end{aligned} \tag{2.1}$$

where $\Omega = 2\sigma^2$, is the mean square value of the received signal amplitude.

2.1.2 Rician Distribution

When a strong LOS path exists between the transmitter and receiver in addition to many weaker random multipath signal components, the randomness of the received signal amplitude is modeled using the Rician distribution whose PDF is given by

$$f(x) = \frac{2x(K+1)}{\Omega} \exp\left(-K - \frac{(K+1)x^2}{\Omega}\right) I_0\left(2x\sqrt{\frac{K(K+1)}{\Omega}}\right), \; x \geq 0 \tag{2.2}$$

where $K = A^2/(2\sigma^2)$ is the Rician factor defined as the ratio of the LOS power A^2 to the scattered power $2\sigma^2$, the average amplitude power is denoted by $\Omega = \mathrm{E}[X^2] = A^2 + 2\sigma^2$ where $\mathrm{E}[\cdot]$ denotes the expectation of a RV, and $I_\nu(\cdot)$ is the νth-order modified Bessel function of the first kind defined as $I_\nu(x) = \sum_{k=0}^{\infty} \frac{(x/2)^{\nu+2k}}{k!\Gamma(\nu+k+1)}$ where $\Gamma(\cdot)$ is the Gamma function defined as $\Gamma(x) = \int_0^\infty t^{x-1} e^{-t} dt$ [26, eq. (8.310.1)]. As the strength of the dominant signal diminishes, i.e. $K = 0$, the Rician distribution specializes to a Rayleigh distribution. As the value of K becomes large, the fading effect tends to vanish.

2.1.3 Nakagami-*m* Distribution

Introduced by Nakagami in the early 1940's [27], the Nakagami-*m* distribution is a versatile distribution used to model multipath fading in wireless channels. Empirical data show that the Nakagami-*m* fading model often gives the best fit to land-mobile and indoor-mobile multipath propagation [2]. The PDF of the Nakagami-*m* distribution is given by

$$f(x) = \frac{2}{\Gamma(m)} \left(\frac{m}{\Omega}\right)^m x^{2m-1} \exp\left(-\frac{mx^2}{\Omega}\right), \; x \geq 0, m \geq \frac{1}{2} \tag{2.3}$$

where Ω is the mean square value of the amplitude. The fading severity parameter m is defined as $\Omega^2/\mathrm{E}[(X^2-\Omega)^2]$. Beyond its empirical justification, the Nakagami-*m* distribution is often used for the following reasons. First, the Nakagami-*m* distribution can be used to model fading conditions more or less severe than Rayleigh fading. When $m = 1$, the Nakagami-*m* distribution becomes the Rayleigh distribution. When $m = 0.5$, it becomes a one-sided Gaussian distribution. As the value of the parameter m increases, the fading severity decreases. Second, the Rician distribution can be approximated by the Nakagami distribution with $K = \sqrt{m^2 - m}/(m - \sqrt{m^2 - m})$ and $m = (K+1)^2/(2K+1)$ for $m > 1$ [3].

The corresponding squared Nakagami-m fading amplitude has a Gamma PDF as

$$f(x) = \frac{1}{\Gamma(m)} \left(\frac{m}{\Omega}\right)^m x^{m-1} \exp\left(-\frac{mx}{\Omega}\right),\ x \geq 0, m \geq \frac{1}{2}. \tag{2.4}$$

2.2 Diversity Combining Techniques

Diversity techniques were introduced to overcome the detrimental effects of multipath fading on wireless communication systems. The principle of diversity techniques is that, if several copies of the same information bearing signal are available and they all experience independent fading, then the probability that all copies are in deep fading simultaneously is small. If signal copies are appropriately combined at the receiver end, one can reduce the effect of multipath fading and improve the performance of wireless communication systems.

There are several known methods to obtain the independent copies of the signal: space diversity, frequency diversity and time diversity. Among them, space diversity is widely used because it is simple to implement and requires no additional bandwidth. In this thesis, we focus only on diversity in the spatial domain with multi-branch reception. The structure of multi-branch diversity combining is shown in Fig. 2.1 where r_i denotes the received signal in the i-th branch, h_i is the channel fading amplitude, φ_i is the corresponding phase, d is the transmitted data symbol, n_i is the complex additive white Gaussian noise (AWGN) in the i-th branch, and w_i is the weighting factor.

The three commonly used multi-branch reception schemes are MRC, SC, and EGC. They are briefly described in the following subsections.

2.2.1 Maximal Ratio Combining

In the maximal ratio combining mechanism, the weighting factors are the complex conjugation of the channel gains, i.e., $w_i = h_i e^{j\varphi_i}$. Therefore, the combiner eliminates the influence

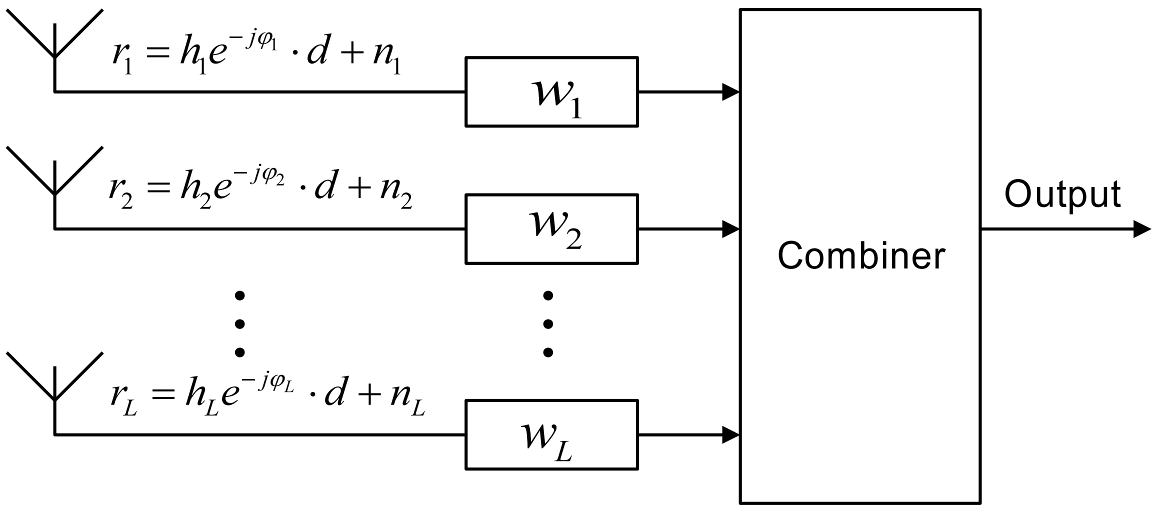

Figure 2.1: Multi-branch diversity combining receiver.

of random phase, which is induced by multipath fading, on the output signal. The combiner amplifies the strong signals and attenuates the weak ones to maximize the instantaneous output SNR at the combiner. Assuming the noise components of the input branches are mutually independent, the output signal of maximal ratio combiner is

$$r_{MRC} = \sum_{i=1}^{L} w_i r_i = \sum_{i=1}^{L} h_i^2 d + h_i e^{j\varphi_i} n_i \tag{2.5}$$

and the instantaneous output SNR γ_{MRC} is given by

$$\gamma_{MRC} = \frac{(\sum_{i=1}^{L} h_i^2)^2 E_S}{(\sum_{i=1}^{L} h_i^2) N_0} = \sum_{i=1}^{L} \frac{h_i^2 E_S}{N_0} = \sum_{i=1}^{L} \gamma_i \tag{2.6}$$

where E_S is the average symbol energy of the transmitted data symbol, N_0 is the power spectral density (PSD) of complex AWGN in the i-th branch, and $\gamma_i = \frac{h_i^2 E_S}{N_0}$ denotes the instantaneous SNR of the i-th branch.

MRC is the optimal diversity combiner in the sense of maximizing the combiner output SNR, in the absence of other interfering sources [28]. However, MRC is also known for having the highest complexity to implement due to the fact that phase-lock and amplitude weighting must be performed.

2.2.2 Equal Gain Combining

In equal gain combining, the weighting factors have constant amplitude value, but have opposite phase to the channel gains, i.e., $w_i = e^{j\varphi_i}$, which is known as the co-phasing operation. Therefore, the combiner only eliminates the influence of random phase with equal weights. Assuming equal noise powers in all branches, the instantaneous output signal of EGC is given by

$$r_{EGC} = \sum_{i=1}^{L} w_i r_i = \sum_{i=1}^{L} h_i d + e^{j\varphi_i} n_i \tag{2.7}$$

and the instantaneous output SNR γ_{EGC} is given by

$$\gamma_{EGC} = \frac{(\sum_{i=1}^{L} h_i)^2 E_S}{L N_0}. \tag{2.8}$$

In practice, exact estimation of the correct weighting factors for MRC can be difficult. Hence, EGC becomes a practical combining scheme with lower implementation complexity than MRC.

2.2.3 Selection Combining

In selection combining, the combiner only picks one best branch out of the L noisy received signals r_i $(i = 1, \cdots, L)$. The weighting factor for the selected branch is unity and the other weighting factors are zero. Suppose all branches have the same noise power spectral density N_0. Then the output of SC can be expressed as

$$r_{SC} = r_{index(max\{h_i\}_{i=1}^{L})} \tag{2.9}$$

where $index(y_i)$ denotes the index i corresponding to y_i. Then the instantaneous output SNR γ_{SC} is given by

$$\gamma_{SC} = \max\{\gamma_i\}_{i=1}^{L} \tag{2.10}$$

where $\gamma_i = \frac{h_i^2 E_S}{N_0}$ denotes the instantaneous SNR of the i-th branch. Since SC processes only a single branch, it has a much lower complexity compared to MRC and EGC. However, since SC ignores information provided by other diversity branches, its performance is poorer than EGC and MRC. SC can be used with coherent modulations, noncoherent modulations, and differentially coherent modulations.

2.3 Asymptotic Technique

Let $\gamma = \beta\bar{\gamma}$ be the instantaneous SNR at the output of the diversity combiner, where β is a RV depending on the channel statistics and $\bar{\gamma}$ is the average SNR at the combiner output. Suppose the PDF of β can be approximated by a single polynomial term for $\beta \to 0^+$ as $f(\beta) = c\beta^t + o(\beta^t)$.[1]

For coherent modulation with conditional SER $p_e(\beta) = pQ\left(\sqrt{q\beta\bar{\gamma}}\right)$, the average SER for large SNR is given by [25]

$$P_e = \frac{2^t c\Gamma\left(t+\frac{3}{2}\right)p}{\sqrt{\pi}\,(t+1)\,(q\bar{\gamma})^{t+1}} + o\left(\frac{1}{\bar{\gamma}^{t+1}}\right). \tag{2.11}$$

Many coherent modulation schemes, such as binary phase shift keying (BPSK), M-ary phase shift keying (M-PSK), M-ary pulse amplitude modulation (M-PAM) and M-ary quadrature amplitude modulation (M-QAM), have conditional SERs of the form $p_e(\beta) = pQ\left(\sqrt{q\beta\bar{\gamma}}\right)$, and the corresponding values of p and q are tabulated in Table 2.1.

To the author's best knowledge, an asymptotic error rate expression for noncoherent modulation in large SNR regions has not been derived. We present this result in the following

[1] We write a function $p(x)$ as $o(x)$ if $\lim_{x\to 0^+} p(x)/x = 0$.

proposition.

Proposition 1: For noncoherent modulation with conditional symbol error rate of the form $p_e(\beta) = p\exp(-q\beta\bar{\gamma})$, the error rate at large SNR can be expressed as

$$P_e = \frac{c\Gamma(t+2)\,p}{(t+1)\,(q\bar{\gamma})^{t+1}} + o\left(\frac{1}{\bar{\gamma}^{t+1}}\right) \tag{2.12}$$

where p and q are constants related to specific modulation formats.

The proof of (2.12) is given in Appendix A. The values of p and q for noncoherent modulations, like binary noncoherent frequency shift keying (BNCFSK) and binary differential phase shift keying (BDPSK), are tabulated in Table 2.1.

Therefore, to compute the asymptotic SER at large SNR, one needs to determine the parameters c and t from the PDF of β, or, from the MGF of β when $s \to \infty$. Another approach is to consider the square root of γ at the output of the diversity combiner. Let $h = \sqrt{\gamma} = \sqrt{\beta\bar{\gamma}}$. From the PDF of β, with a change of variable, it is straightforward to obtain the PDF of γ as

$$f(\gamma) = c\frac{\gamma^t}{\bar{\gamma}^{t+1}} + o\left(\frac{\gamma^t}{\bar{\gamma}^{t+1}}\right). \tag{2.13}$$

The PDF of h is

$$f(h) = 2c\frac{h^{2t+1}}{\bar{\gamma}^{t+1}} + o\left(\frac{h^{2t+1}}{\bar{\gamma}^{t+1}}\right) \tag{2.14}$$

and the corresponding MGF of h can be expressed as

$$\mathscr{M}_h(s) = \frac{2c\Gamma(2t+2)}{\bar{\gamma}^{t+1}s^{2t+2}} + o\left(\frac{1}{\bar{\gamma}^{t+1}s^{2t+2}}\right). \tag{2.15}$$

Therefore, one can simply obtain the asymptotic SER by extracting the parameters c and t from (2.13) to (2.15) in the frequency domain.

On the other hand, the asymptotic SER can also be approximated by (see, e.g., [25], [29])

$$P_e = (G_c \cdot \bar{\gamma})^{-G_d} + o\left(\frac{1}{\bar{\gamma}^{G_d}}\right) \tag{2.16}$$

Table 2.1: Parameters p and q for different coherent and noncoherent modulation schemes

Modulation Scheme	Conditional SER	p	q
BPSK	$Q\left(\sqrt{2\gamma}\right)$	1	2
M-PSK $M \geq 4$	$\approx 2Q\left(\sqrt{2\gamma}\sin\frac{\pi}{M}\right)$	2	$2\sin^2\frac{\pi}{M}$
M-PAM	$2(1-\frac{1}{M})Q\left(\sqrt{\frac{6\gamma}{M^2-1}}\right)$	$2(1-\frac{1}{M})$	$\frac{6}{M^2-1}$
M-QAM	$4(1-\frac{1}{\sqrt{M}})Q\left(\sqrt{\frac{3\gamma}{M-1}}\right)$	$4(1-\frac{1}{\sqrt{M}})$	$\frac{3}{M-1}$
BNCFSK	$\frac{1}{2}\exp\left(-\frac{1}{2}\gamma\right)$	$\frac{1}{2}$	$\frac{1}{2}$
BDPSK	$\frac{1}{2}\exp\left(-\gamma\right)$	$\frac{1}{2}$	1

where G_c is the coding gain, and G_d is the diversity order. The diversity order G_d determines the slope of the SER versus average SNR curve, at high SNR, in a log-log scale. G_c (in decibels) determines the shift of the curve in SNR relative to a benchmark SER curve of $\left(\bar{\gamma}^{-G_d}\right)$. Comparing (2.16) with (2.11) and (2.12) respectively, we observe that $G_d = t+1$ for both coherent and noncoherent modulation, $G_c = q\left[\frac{2^t cp\Gamma\left(t+\frac{3}{2}\right)}{\sqrt{\pi}(t+1)}\right]^{-\frac{1}{t+1}}$ for coherent modulation, and $G_c = q\left[\frac{cp\Gamma(t+2)}{t+1}\right]^{-\frac{1}{t+1}}$ for noncoherent modulation.

2.4 Construction of Multiple Correlated Nakagami-m RVs

In this section, we present a framework to obtain a single integral representation for multiple Nakagami-m distributions with a specified correlation matrix. The joint PDF of correlated Nakagami-m RVs is expressed explicitly in terms of single integral solutions. A remarkable feature of these expressions is that the computational complexity reduces to a single integral computation for an arbitrary number of dimensions. The basic idea for the construction of multiple correlated Nakagami-m RVs is that a set of equally correlated complex Gaussian RVs can be obtained by linearly combining a set of independent Gaussian RVs [30]. The original construction approach was proposed in [17] to obtain the CDF of L-branch SC output SNR in equally correlated Nakagami-m fading. In [14], this approach was used to evaluate the performance of diversity combiners with positively correlated branches.

2.4.1 Construction of Multiple Correlated Nakagami-*m* RVs

Similar to [17, eq. (5)], [30] for integer m we express the L correlated Nakagami-m RVs through Lm zero-mean complex Gaussian RVs by

$$G_{il} = \sigma_i \left(\sqrt{1-\rho_i} X_{il} + \sqrt{\rho_i} X_{0l} \right) + j\sigma_i \left(\sqrt{1-\rho_i} Y_{il} + \sqrt{\rho_i} Y_{0l} \right) \tag{2.17}$$

for $i = 1, \cdots, L$ and $l = 1, \cdots, m$, where $j^2 = -1$, $0 \le \rho_i \le 1$, and X_{0l}, X_{il}, Y_{0l} and Y_{il} are independent Gaussian RVs with distribution $\mathcal{N}(0, 1/2)$. That is, for any $u, v \in \{0, 1, \cdots, L\}$, and $l, n \in \{1, \cdots, m\}$, $\mathrm{E}[X_{ul} Y_{vn}] = 0$, $\mathrm{E}[X_{ul} X_{vn}] = \mathrm{E}[Y_{ul} Y_{vn}] = \delta_{u,v}\delta_{l,n}/2$, where $\delta_{u,v}$ is the Kronecker delta function.

Let R_i denote the summation of the absolute square of G_{il}, i.e., $R_i = \sum_{l=1}^{m} |G_{il}|^2$. Then, it can be shown R_i is the sum of squares of m independent Rayleigh envelopes with central chi-square distribution $\chi_{2m}(0, \sigma_i^2/2)$ [14]. The cross-correlation between R_i and R_k can be shown to be

$$\rho_{R_i,R_k} = \frac{\mathrm{E}[R_i R_k] - \mathrm{E}[R_i]\,\mathrm{E}[R_k]}{\sqrt{\mathrm{Var}[R_i]\,\mathrm{Var}[R_k]}} = \rho_i \rho_k, \quad i \neq k \tag{2.18}$$

where $\mathrm{Var}[\cdot]$ denotes the variance of a RV. The proof of (2.18) is given in Appendix B.

Let $H_i = \sqrt{R_i}$, then it can be shown $H_1, H_2, \cdots, H_L$ are L correlated Nakagami-m RVs with identical fading parameter m and mean-square value $m\sigma_i^2$. The relationship between the correlation of H_i and H_k and the correlation of R_i and R_k, denoted by ρ_{H_i,H_k} and ρ_{R_i,R_k} respectively, is [27]

$$\rho_{H_i,H_k} = \frac{F\left(-\frac{1}{2}, -\frac{1}{2}; m; \rho_{R_i,R_k}\right) - 1}{\psi(m) - 1} \tag{2.19}$$

where $\psi(m) = \Gamma(m)\Gamma(m+1)/\Gamma^2(m+1/2)$ and $F(\cdot)$ is the hypergeometric function defined as $F(a,b;c;z) = \frac{\Gamma(c)}{\Gamma(a)\Gamma(b)} \sum_{n=0}^{\infty} \frac{\Gamma(a+n)\Gamma(b+n)}{\Gamma(c+n)} \frac{z^n}{n!}$ [31, eq. (15.1.1)].

2.4.2 Joint PDF of Multiple Correlated Nakagami-m RVs

Let $Z = \sum_{l=1}^{m}\left(X_{0l}^2 + Y_{0l}^2\right)$. When $X_{0l} = x_{0l}$ and $Y_{0l} = y_{0l}$ $(l = 1, \cdots, m)$ are fixed, the real and imaginary parts of G_{il} have equal variance of $\sigma_i^2(1-\rho_i)/2$ and means $\sigma_i\sqrt{\rho_i}x_{0l}$ and $\sigma_i\sqrt{\rho_i}y_{0l}$, respectively. Therefore, $R_1, R_2, \cdots, R_L$ are independent noncentral chi-square RVs with distribution $\chi_{2m}(\sqrt{\rho_i\sum_{l=1}^{m}\left(x_{0l}^2 + y_{0l}^2\right)}, \sigma_i^2(1-\rho_i)/2)$ and whose marginal CDF is given by [29, eq. (2-1-124)]

$$F\left(r_i|z\right) = \Pr\left(R_i \le r_i|z\right) = 1 - Q_m\left(\sqrt{\frac{2z\rho_i}{1-\rho_i}}, \sqrt{\frac{2r_i}{\sigma_i^2\left(1-\rho_i\right)}}\right) \tag{2.20}$$

where $Q_m\left(\cdot,\cdot\right)$ denotes the m-th order Marcum Q-function defined as $Q_m(\alpha,\beta) = \int_{\beta}^{\infty} x\left(\frac{x}{\alpha}\right)^{m-1} e^{-\frac{x^2+\alpha^2}{2}} I_{m-1}\left(\alpha x\right)dx$ [32]. The joint marginal CDF of $R_1, \cdots, R_L$ is given by

$$F\left(r_1, r_2, \cdots, r_L|z\right) = \prod_{i=1}^{L}\left[1 - Q_m\left(\sqrt{\frac{2z\rho_i}{1-\rho_i}}, \sqrt{\frac{2r_i}{\sigma_i^2\left(1-\rho_i\right)}}\right)\right]. \tag{2.21}$$

$Z = \sum_{l=1}^{m}\left(X_{0l}^2 + Y_{0l}^2\right)$ follows a central chi-square distribution $\chi_{2m}(0, 1/2)$ and its PDF is given by

$$f\left(z\right) = \frac{z^{m-1}e^{-z}}{\Gamma\left(m\right)},\ z \ge 0. \tag{2.22}$$

Averaging the joint marginal CDF in (2.21) with respect to the PDF of Z, the joint CDF of $R_1, R_2, \cdots, R_L$ becomes

$$F\left(r_1, r_2, \cdots, r_L\right) = \frac{1}{\Gamma\left(m\right)}\int_0^{\infty}\prod_{i=1}^{L}\left[1 - Q_m\left(\sqrt{\frac{2z\rho_i}{1-\rho_i}}, \sqrt{\frac{2r_i}{\sigma_i^2\left(1-\rho_i\right)}}\right)\right]z^{m-1}e^{-z}dz. \tag{2.23}$$

Taking partial derivatives of (2.23) with respect to $r_1, r_2, \cdots, r_L$, one can obtain the joint PDF of $R_1, R_2, \cdots, R_L$ as follows

$$f(r_1, r_2, \cdots, r_L) = \frac{1}{\Gamma(m)} \int_0^\infty \prod_{i=1}^{L} \frac{1}{\sigma_i^2(1-\rho_i)} \left(\frac{r_i}{z\rho_i\sigma_i^2}\right)^{\frac{m-1}{2}} \exp\left[-\frac{r_i}{\sigma_i^2(1-\rho_i)}\right] \times I_{m-1}\left(\frac{2}{1-\rho_i}\sqrt{\frac{z\rho_i r_i}{\sigma_i^2}}\right) z^{m-1} e^{-\left(1+\sum_{i=1}^{L}\frac{\rho_i}{1-\rho_i}\right)z} dz. \tag{2.24}$$

Eqns. (2.23) and (2.24) essentially are the joint CDF and PDF of L correlated Gamma RVs respectively, and will be useful in studying the asymptotic performance of SC.

Using variable transformation, we can obtain the joint PDF of $H_1, H_2, \cdots, H_L$ as

$$f(h_1, h_2, \cdots, h_L) = \frac{1}{\Gamma(m)} \int_0^\infty \prod_{i=1}^{L} \frac{2h_i}{\sigma_i^2(1-\rho_i)} \left(\frac{h_i^2}{z\rho_i\sigma_i^2}\right)^{\frac{m-1}{2}} \exp\left[-\frac{h_i^2}{\sigma_i^2(1-\rho_i)}\right] \times I_{m-1}\left(\frac{2}{1-\rho_i}\sqrt{\frac{z\rho_i h_i^2}{\sigma_i^2}}\right) z^{m-1} e^{-\left(1+\sum_{i=1}^{L}\frac{\rho_i}{1-\rho_i}\right)z} dz. \tag{2.25}$$

The proof of (2.25) is given in Appendix C. Eqn. (2.25) is the joint the PDF of L correlated Nakagami-m RVs and will be useful in studying the asymptotic performance of EGC.

Chapter 3

Asymptotic Performance Analysis of SC over Arbitrarily Correlated Nakagami-*m* Fading Channels

3.1 Introduction

The generalized Marcum Q-function has a long history in signal processing literature, especially in the analysis of target detection by pulsed radars with single or multiple observations [32]. This special function is also frequently used in the performance analysis involving noncoherent and differential detection of multichannel narrowband signals over fading channels [2], [29]. The generalized Marcum Q-function is given by [32]

$$Q_v(\alpha,\beta) = \int_{\beta}^{\infty} x\left(\frac{x}{\alpha}\right)^{v-1} e^{-\left(x^2+\alpha^2\right)/2} I_{v-1}\left(\alpha x\right) dx \tag{3.1}$$

where α and β are non-negative real numbers, and v is a positive real number. Although v can take any positive real number, when v is a positive integer m, $Q_m(\alpha,\beta)$ is the complementary cumulative distribution function of a noncentral chi-square RV with $2m$ degrees of freedom [33].

Because of its importance, the generalized Marcum Q-function has been the subject of considerable research over the past several decades. The precise computation of $Q_v(\alpha,\beta)$ can be difficult especially for large α and v values, because the integral in (3.1) involves the modified Bessel function of the first kind [34]. In order to calculate the generalized Marcum Q-function, power series expansion methods were used in [35–37] and the Neuman series expansion method was proposed in [38]. Since direct computation of (3.1) is difficult, various alternative representations of $Q_v(\alpha,\beta)$ were proposed. For example, several integral forms of $Q_v(\alpha,\beta)$ were developed in [39–45] and the references therein. During the past decade, several upper and lower bounds were proposed for the generalized Marcum Q-function [46–55]. Most of these bounds were obtained by utilizing the bounds of the integrand in (3.1) or by changing the integral region via a geometric interpretation of the functions.

In this thesis, using a series expansion of the modified Bessel function of the first kind $I_{m-1}(x)$ we present a new series representation of $Q_m(\alpha,\beta)$ in terms of the incomplete gamma function $\gamma(m,x)$ and obtain a simple accurate approximation of $Q_m(\alpha,\beta)$ when $\beta \to 0^+$. Utilizing this approximation of $Q_m(\alpha,\beta)$, we study the asymptotic performance of selection combining over arbitrarily correlated Nakagami-m channels. Of practical value, we derive new compact analytical results that can be used to provide rapid and accurate error rate and outage probability estimation. Of theoretical interest, we reveal some physical insights into the transmission characteristics of SC over correlated Nakagami-m channels, and in particular, how the branch power covariance coefficient matrix can influence the average error rate and outage probability in large SNR regions.

The rest of this chapter is organized as follows. In Section 3.2, an alternative series representation and a new approximation of $Q_m(\alpha,\beta)$ when $\beta \to 0^+$ are presented. In Section 3.3, the PDF of L-branch SC output SNR near its origin over arbitrarily correlated Nakagami-m fading channels is derived. Section 3.4 derives the asymptotic error rate and outage probability of SC. Section 3.5 discusses some important insights and provides some numerical results.

3.2 A Series Representation of $Q_m(\alpha,\beta)$

We first present a new series representation of $Q_m(\alpha,\beta)$ as follows.

Proposition 2: The generalized Marcum Q-function can be written as

$$Q_m(\alpha,\beta) = 1 - e^{-\frac{\alpha^2}{2}} \sum_{k=0}^{\infty} \frac{\alpha^{2k}}{\Gamma(m+k)\,k!\cdot 2^k}\gamma\left(m+k,\frac{\beta^2}{2}\right) \tag{3.2}$$

where $\gamma(\cdot,\cdot)$ is the incomplete gamma function defined as $\gamma(m,z) = \int_0^z t^{m-1}e^{-t}dt$ [26, (8.350.1)].

Proof: By [33, eq. (5)-(8)], for integer-valued m the generalized Marcum Q-function can be expressed as

$$\begin{aligned} Q_m(\alpha,\beta) &= \int_{\beta}^{\infty} x\left(\frac{x}{\alpha}\right)^{m-1} e^{-\left(x^2+\alpha^2\right)/2} I_{m-1}(\alpha x)\,dx \\ &= 1 - \int_0^{\beta} x\left(\frac{x}{\alpha}\right)^{m-1} e^{-\left(x^2+\alpha^2\right)/2} I_{m-1}(\alpha x)\,dx. \end{aligned} \tag{3.3}$$

For m-th order modified Bessell function of the first kind, its series expansion can be represented as [26, (8.445)]

$$I_m(z) = \sum_{k=0}^{\infty} \frac{1}{\Gamma(m+k+1)\,k!}\left(\frac{z}{2}\right)^{m+2k}. \tag{3.4}$$

Substituting (3.4) into (3.3), we have

$$\begin{aligned} &\int_0^{\beta} x\left(\frac{x}{\alpha}\right)^{m-1} e^{-\left(x^2+\alpha^2\right)/2} I_{m-1}(\alpha x)\,dx \\ &= \alpha^{1-m} e^{-\frac{\alpha^2}{2}} \sum_{k=0}^{\infty} \frac{1}{\Gamma(m+k)\,k!}\left(\frac{\alpha}{2}\right)^{m+2k-1} \int_0^{\beta} x^{2m+2k-1} e^{-\frac{x^2}{2}}\,dx \\ &= e^{-\frac{\alpha^2}{2}} \sum_{k=0}^{\infty} \frac{\alpha^{2k}}{\Gamma(m+k)\,k!\cdot 2^k}\cdot\gamma\left(m+k,\frac{\beta^2}{2}\right) \end{aligned} \tag{3.5}$$

and (3.2) follows immediately.

Using the series expression of the incomplete gamma function $\gamma(u,y) = \sum_{n=0}^{\infty} \frac{(-1)^n y^{u+n}}{n!(u+n)}$

[26, (8.354.1)], we can rewrite $Q_m(\alpha,\beta)$ as

$$Q_m(\alpha,\beta) = 1 - e^{-\frac{\alpha^2}{2}} \sum_{k=0}^{\infty} \frac{\alpha^{2k}}{\Gamma(m+k)\, k! \cdot 2^k} \sum_{n=0}^{\infty} \frac{(-1)^n \left(\frac{\beta^2}{2}\right)^{m+k+n}}{(m+k+n)\cdot n!}. \tag{3.6}$$

An immediate consequence of (3.6) is that when $\beta \to 0^+$, the m-th order Marcum Q-function $Q_m(\alpha,\beta)$ can be approximated as

$$Q_m(\alpha,\beta) = 1 - \frac{\beta^{2m}}{2^m \cdot m!} \exp\left(-\frac{\alpha^2}{2}\right) + o\left(\beta^{2m}\right). \tag{3.7}$$

To demonstrate the accuracy of the above approximation, we calculate the exact values of $Q_m(\alpha,\beta)$ using the function NCX2CDF provided by Matlab and compare them with the approximate values obtained from (3.7) for different values of α and β. The numerical results are compared in Table 3.1. From Table 3.1, we can observe that the relative error becomes small when $\beta \to 0^+$, and therefore we conclude that the small argument approximation of the Marcum Q-function is highly accurate.

3.3 PDF of SC Output SNR Over Correlated Nakagami-*m* Fading Channels

3.3.1 System Model

Assume that there are L available diversity branches experiencing frequency-nonselective and slow Nakagami-m fading with fading parameter m taking the same positive integer value. Let H_i be the instantaneous channel fading amplitude on the i-th branch, E_S be the average symbol energy of the transmitted data symbol, and let N_0 be the PSD of complex AWGN in the i-th branch. The instantaneous SNR of the i-th diversity branch, γ_i, is defined as

$$\gamma_i = |H_i|^2 \frac{E_S}{N_0} \tag{3.8}$$

Table 3.1: The exact and approximate values of $Q_m(\alpha, \beta)$ for different values of α and β

α	β	Exact value	Approximate value	Relative error
0.1	0.1	0.999996887986722	0.999987562344010	9.325×10^{-6}
	0.05	0.999999805256228	0.999999222646501	5.826×10^{-7}
	0.01	0.999999999688286	0.999999998756234	9.32×10^{-10}
	0.005	0.999999999980518	0.999999999922265	5.825×10^{-11}
	0.001	0.999999999999969	0.999999999999876	9.314×10^{-14}
1	0.1	0.999997569793885	0.999992418366754	5.151×10^{-6}
	0.05	0.999999847945917	0.999999526147922	3.217×10^{-7}
	0.01	0.999999999756628	0.999999999241837	5.147×10^{-10}
	0.005	0.999999999984789	0.999999999952615	3.217×10^{-11}
	0.001	0.999999999999976	0.999999999999924	5.151×10^{-14}
5	0.1	0.999999993945953	0.999999999953417	6.007×10^{-9}
	0.05	0.999999999622624	0.999999999997089	3.744×10^{-10}
	0.01	0.999999999999397	0.999999999999995	5.986×10^{-13}
	0.005	0.999999999999962	1.000000000000000	3.741×10^{-14}
	0.001	0.9999999999999999	1	1.11×10^{-16}

and the average SNR of the i-th diversity branch, Γ_i, is given by

$$\Gamma_i = \mathrm{E}\left[|H_i|^2\right]\frac{E_S}{N_0}. \tag{3.9}$$

Recall from Chapter 2 that for SC, the instantaneous SNR at the output of the selection combiner is given by

$$\gamma_{SC} = \max_{i=1,\cdots,L}\gamma_i. \tag{3.10}$$

3.3.2 PDF of SC Output SNR

We now use the method described in Chapter 2 to construct correlated Nakagami-m RVs $H_1, H_2, \ldots, H_L$. Then the instantaneous SNR of the i-th diversity branch is $\gamma_i = R_i\frac{E_S}{N_0}$. Let $\mathbf{R}$ denote the branch power covariance coefficient matrix, whose (ik)-th element $(\mathbf{R})_{ik}$ is defined as

$$(\mathbf{R})_{ik} = \frac{\mathrm{E}[\gamma_i\gamma_k] - \mathrm{E}[\gamma_i]\,\mathrm{E}[\gamma_k]}{\sqrt{\mathrm{Var}[\gamma_i]\,\mathrm{Var}[\gamma_k]}}. \tag{3.11}$$

Using (2.18), we can show that

$$(\mathbf{R})_{ik} = \begin{cases} \rho_{R_i,R_k} = \rho_i\rho_k, & i \neq k \\ 1, & i = k \end{cases}. \tag{3.12}$$

This model simplifies to the equally correlated case when $\rho_i = \rho_k$. By the symmetry property of $\mathbf{R}$, ρ_i and ρ_k can be uniquely determined by

$$\rho_i = \sqrt{\frac{(\mathbf{R})_{il}(\mathbf{R})_{in}}{(\mathbf{R})_{ln}}} \tag{3.13}$$

and

$$\rho_k = \sqrt{\frac{(\mathbf{R})_{kl}(\mathbf{R})_{kn}}{(\mathbf{R})_{ln}}} \tag{3.14}$$

when $n, l \neq i, n, l \neq k, l \neq n$.

If we define $\mathbf{M}$ as the matrix whose (ik)-th entry is given by

$$(\mathbf{M})_{ik} = \sqrt{(\mathbf{R})_{ik}}. \tag{3.15}$$

Express $\mathbf{M}$ as a rank-one updated matrix $\mathbf{M} = \mathbf{S} + \mathbf{u}\mathbf{u}^T$, where $\mathbf{S} = \text{diag}(1-\rho_1, \cdots, 1-\rho_L)$ and $\mathbf{u} = [\sqrt{\rho_1}, \sqrt{\rho_2}, \cdots, \sqrt{\rho_L}]$. Using [56, eq. (6.2.3)], we can obtain the determinant of matrix $\mathbf{M}$ as

$$\det(\mathbf{M}) = \det(\mathbf{S})\left(1 + \mathbf{u}^T\mathbf{S}^{-1}\mathbf{u}\right) = \left[1 + \sum_{i=1}^{L} \frac{\rho_i}{1-\rho_i}\right] \prod_{i=1}^{L} (1-\rho_i). \tag{3.16}$$

Following the construction of $H_1, H_2, \ldots, H_L$ described in Chapter 2, we can obtain the mean square value of H_i as $\text{E}\left[|H_i|^2\right] = m\sigma_i^2$ and the average SNR of the i-th diversity branch as $\Gamma_i = m\sigma_i^2 \frac{E_S}{N_0}$. Since the instantaneous SNR of the i-th diversity branch is $\gamma_i = R_i \frac{E_S}{N_0}$, we can express γ_i in terms of as Γ_i, i.e., $\gamma_i = \frac{R_i}{m\sigma_i^2}\Gamma_i$. By (3.10), the CDF of the SC output SNR γ_{SC} can be written as

$$\begin{aligned}
F_{\gamma_{SC}}(\gamma) &= \Pr(\gamma_{sc} \le \gamma) \\
&= \Pr(\gamma_1 \le \gamma, \cdots, \gamma_L \le \gamma) \\
&= \Pr\left(\frac{R_1}{m\sigma_1^2}\Gamma_1 \le \gamma, \cdots, \frac{R_L}{m\sigma_L^2}\Gamma_L \le \gamma\right) \\
&= \Pr\left(R_1 \le \frac{m\sigma_1^2}{\Gamma_1}\gamma, \cdots, R_L \le \frac{m\sigma_L^2}{\Gamma_L}\gamma\right).
\end{aligned} \tag{3.17}$$

By the joint CDF of $R_1, R_2, \cdots, R_L$ given in (2.23), we can obtain

$$F_{\gamma_{SC}}(\gamma) = \frac{1}{\Gamma(m)} \int_0^{\infty} \prod_{i=1}^{L} \left[1 - Q_m\left(\sqrt{\frac{2\rho_i z}{1-\rho_i}}, \sqrt{\frac{2m\gamma}{\Gamma_i(1-\rho_i)}}\right)\right] z^{m-1} e^{-z} dz. \tag{3.18}$$

Eqn. (3.18) essentially generalizes the results in [17] and [14] to arbitrarily correlated SC over branches with different average SNR values.

It is seen from (3.18) that the second parameter of the generalized Marcum Q-function approaches zero when $\gamma \to 0^+$, or when the CDF is near its origin. Using (3.7), we can obtain the asymptotic CDF of the SC output SNR as

$$F_{\gamma_{SC}}(\gamma) = \frac{m^{mL}}{\left[\Gamma(m+1)\right]^L \det^m(\mathbf{M})} \frac{\gamma^{mL}\bar{\gamma}^{mL}}{\prod_{i=1}^{L}\Gamma_i^m \bar{\gamma}^{mL}} + o\left(\frac{\gamma^{mL}}{\bar{\gamma}^{mL}}\right). \tag{3.19}$$

Differentiating (3.19) with respect to γ, we obtain the PDF of instantaneous SNR at the output of the SC as

$$f_{\gamma_{SC}}(\gamma) = \frac{mL\cdot m^{mL}}{\left[\Gamma(m+1)\right]^L \det^m(\mathbf{M})} \frac{\gamma^{mL-1}\bar{\gamma}^{mL}}{\prod_{i=1}^{L}\Gamma_i^m \bar{\gamma}^{mL}} + o\left(\frac{\gamma^{mL-1}}{\bar{\gamma}^{mL}}\right). \tag{3.20}$$

The analytical expression obtained in (3.20) for the PDF of the output SNR near its origin will be useful in studying the asymptotic error rate performance of SC.

3.4 Asymptotic Performance Analysis of SC

Comparing (3.20) with (2.13) in Chapter 2, we observe that

$$t = mL - 1 \tag{3.21}$$

and

$$c = \frac{mL\cdot m^{mL}}{\left[\Gamma(m+1)\right]^L \det^m(\mathbf{M})} \frac{\bar{\gamma}^{mL}}{\prod_{i=1}^{L}\Gamma_i^m}. \tag{3.22}$$

From (3.21), it is obvious that the diversity order G_d is mL.

3.4.1 Asymptotic Error Rate

The asymptotic SER of SC reception with coherent modulation can thus be expressed from (2.11) as

$$P_e^{S,C} = \frac{\Gamma(2mL+1)\, m^{mL} p}{2^{mL+1} q^{mL} \Gamma(mL+1) \left[\Gamma(m+1)\right]^L \det^m(\mathbf{M})} \frac{1}{\prod_{i=1}^{L} \Gamma_i^m} + o\left(\frac{1}{\prod_{i=1}^{L} \Gamma_i^m}\right). \tag{3.23}$$

In the special case when $m = 1$, it can be shown that (3.23) agrees with the asymptotic error rate of SC reception over arbitrarily correlated Rayleigh channels [5, eq. (7)][2]. Similarly, the asymptotic SER of SC reception with noncoherent modulation can be obtained from (2.12) as

$$P_e^{S,N} = \frac{m^{mL} \Gamma(mL+1)\, p}{k^{mL} \left[\Gamma(m+1)\right]^L \det^m(\mathbf{M})} \frac{1}{\prod_{i=1}^{L} \Gamma_i^m} + o\left(\frac{1}{\prod_{i=1}^{L} \Gamma_i^m}\right). \tag{3.24}$$

3.4.2 Asymptotic Outage Probabilities

The outage probability is defined as

$$P_{out}(\gamma_{th}) = \Pr(\gamma < \gamma_{\text{th}}) = \int_0^{\gamma_{\text{th}}} f(\gamma) d\gamma \tag{3.25}$$

where γ_{th} is a predefined outage threshold and $f(\gamma)$ is the PDF of the instantaneous SNR at the output of diversity combiner. Substituting (2.13) into (3.25), one obtains the asymptotic outage probabilities as

$$P_{out}(\gamma_{th}) = \frac{c}{t+1} \left(\frac{\gamma_{th}}{\bar{\gamma}}\right)^{t+1} + o\left(\frac{\gamma_{th}^{t+1}}{\bar{\gamma}^{t+1}}\right). \tag{3.26}$$

[2]When $m = 1$, $\mathbf{M}$ is same as the matrix $\mathbf{M}$ defined in [5].

With the values of t and c obtained in (3.21) and (3.22), we obtain

$$P_{out}^{S}\left(\gamma_{th}\right)=\frac{m^{mL}}{(m!)^{L}\det^{m}(\mathbf{M})}\frac{\gamma_{th}^{mL}}{\prod_{i=1}^{L}\Gamma_{i}^{m}}+o\left(\frac{1}{\prod_{i=1}^{L}\Gamma_{i}^{m}}\right). \quad (3.27)$$

When $m=1$, it can be shown that (3.27) agrees with the asymptotic outage probability of SC reception over arbitrarily correlated Rayleigh channels [5, eq. (14)].

Although we have derived the asymptotic error rate and outage probability expressions (3.23), (3.24) and (3.27) assuming integer fading parameter values, our numerical results suggest these analytical expressions are also valid at least for $m=0.5$.

3.5 Discussions and Numerical Results

3.5.1 Discussions

Since $\det(\mathbf{M})=1$ for independent fading channels, we observe from (3.23) and (3.24) that the asymptotic SER of SC over arbitrarily correlated Nakagami-m fading channels can be expressed in terms of the asymptotic SER over independent Nakagami-m fading channels scaled by a factor $\det^{m}(\mathbf{M})$, i.e.,

$$(P_{e}^{SC})_{asym}=\frac{(P_{e,i}^{SC})_{asym}}{\det^{m}(\mathbf{M})} \quad (3.28)$$

where $(P_{e,i}^{SC})_{asym}$ denotes the asymptotic SER of SC over independent Nakagami-m fading branches. In (3.28), the factor $\det^{m}(\mathbf{M})$, which is less than unity, can be considered as the loss factor due to channel correlation. It should be noted that the simple relationship in (3.28) also holds for MRC over arbitrarily correlated Nakagami-m fading channels [25]. Finally a relationship similar to (3.28) can also be seen for the outage probability from (3.27).

3.5.2 Numerical Results

In this subsection, we present some numerical results of coherent BPSK and noncoherent BDPSK with three-branch SC over correlated Nakagami-m fading channels. We use the method proposed in [57] to generate correlated Nakagami-m RVs. For all the numerical results obtained here, we have assumed three-branch diversity reception with $\Gamma_1 = \Gamma_2 = \Gamma_3$ and $\gamma_{th} = 3$ dB. We use $\tilde{\rho} = [\rho_{\mathbf{1}}, \rho_{\mathbf{2}}, \rho_{\mathbf{3}}]$ to denote a vector whose elements comprise the power covariance coefficient matrix. For comparison, we set $\tilde{\rho}_{\mathbf{1}} = [0.4571, 0.2296, 0.4571]$ and $\tilde{\rho}_{\mathbf{2}} = [0.3968, 0.5265, 0.7861]$. By (3.12) and (3.15), we obtain

$$\mathbf{M}_1 = \begin{pmatrix} 1 & 0.3240 & 0.4571 \\ 0.3240 & 1 & 0.3240 \\ 0.4571 & 0.3240 & 1 \end{pmatrix}$$

and

$$\mathbf{M}_2 = \begin{pmatrix} 1 & 0.4571 & 0.5585 \\ 0.4571 & 1 & 0.6433 \\ 0.5585 & 0.6433 & 1 \end{pmatrix}.$$

It follows that det($\mathbf{M}_1$)= 0.6771 and det($\mathbf{M}_2$)= 0.3937. From (3.28), the determinant inequality $\det(\mathbf{M}_1) > \det(\mathbf{M}_2)$ predicts that more highly correlated fading channels will lead to worse SER performance, as one expects. This is confirmed by the bit error rate (BER) curves shown in Fig. 3.1 and Fig. 3.2 for $m = 0.5$ and $m = 2$ respectively.

Fig. 3.3 and Fig. 3.4 plot the asymptotic and simulated outage probabilities of three-branch SC with matrices $\mathbf{M}_1$ and $\mathbf{M}_2$ for $m = 0.5$ and $m = 2$ respectively. Figs. 3.1- 3.4 indicate that the analytical asymptotic results have excellent agreement with the simulated result in large SNR regions. This implies that the analytical asymptotic results can be used to predict small values of error rate and outage probability accurately for large SNR regions, where Monte Carlo simulation becomes time-consuming. Note that Fig. 3.1 and Fig. 3.3 also suggest that (3.23), (3.24) and (3.27) are also valid at least for $m = 0.5$.

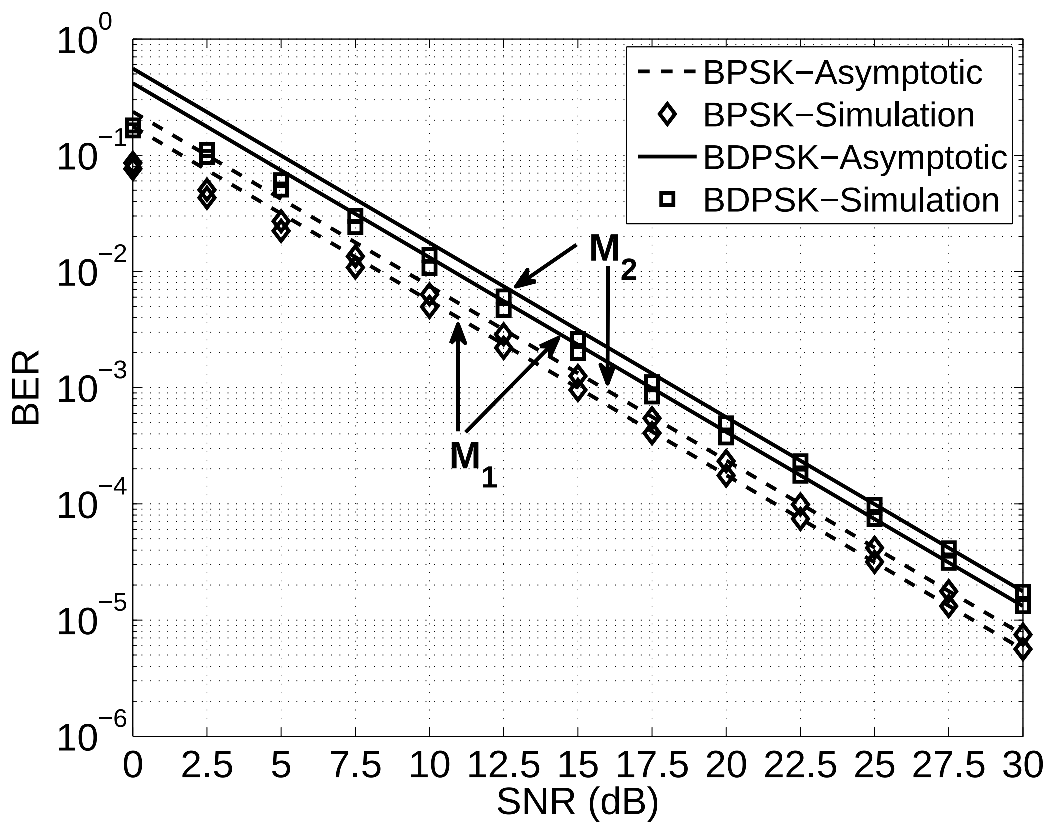

Figure 3.1: The asymptotic and simulated BERs of BPSK and BDPSK for SC over 3-branch correlated Nakagami-m channels with matrices $\mathbf{M}_1$ and $\mathbf{M}_2$ when $m = 0.5$.

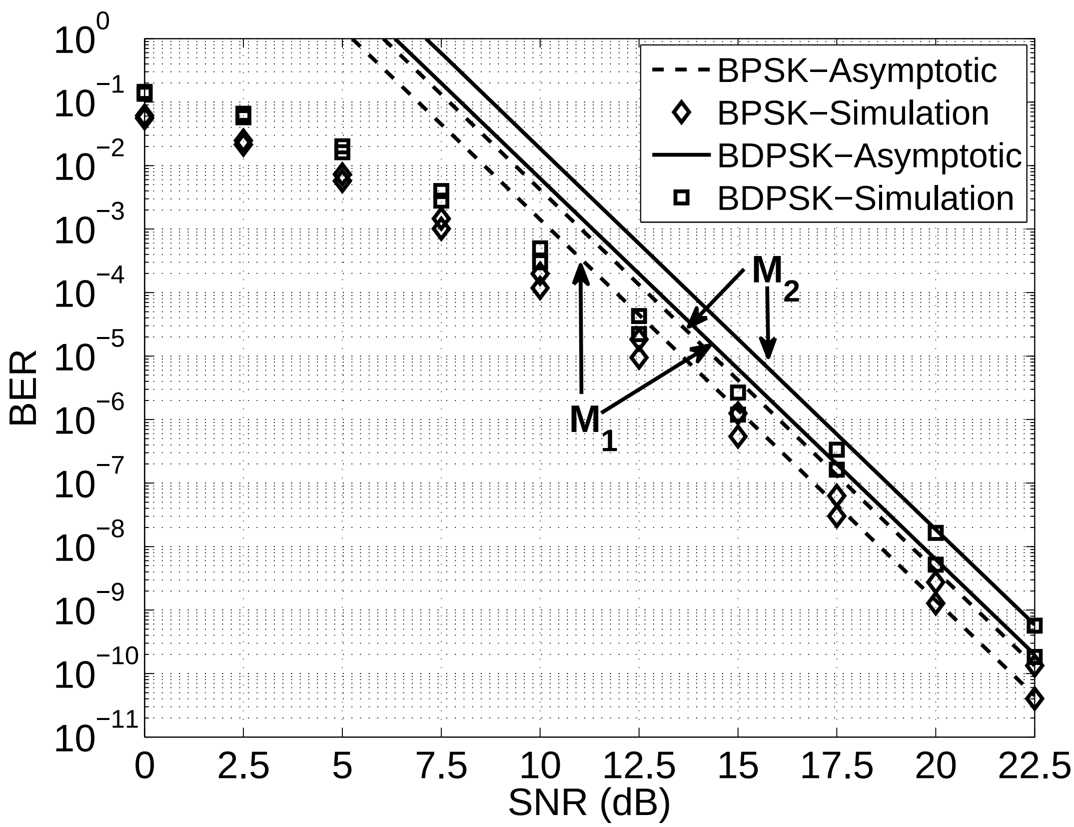

Figure 3.2: The asymptotic and simulated BERs of BPSK and BDPSK for SC over 3-branch correlated Nakagami-m channels with matrices $\mathbf{M}_1$ and $\mathbf{M}_2$ when $m = 2$.

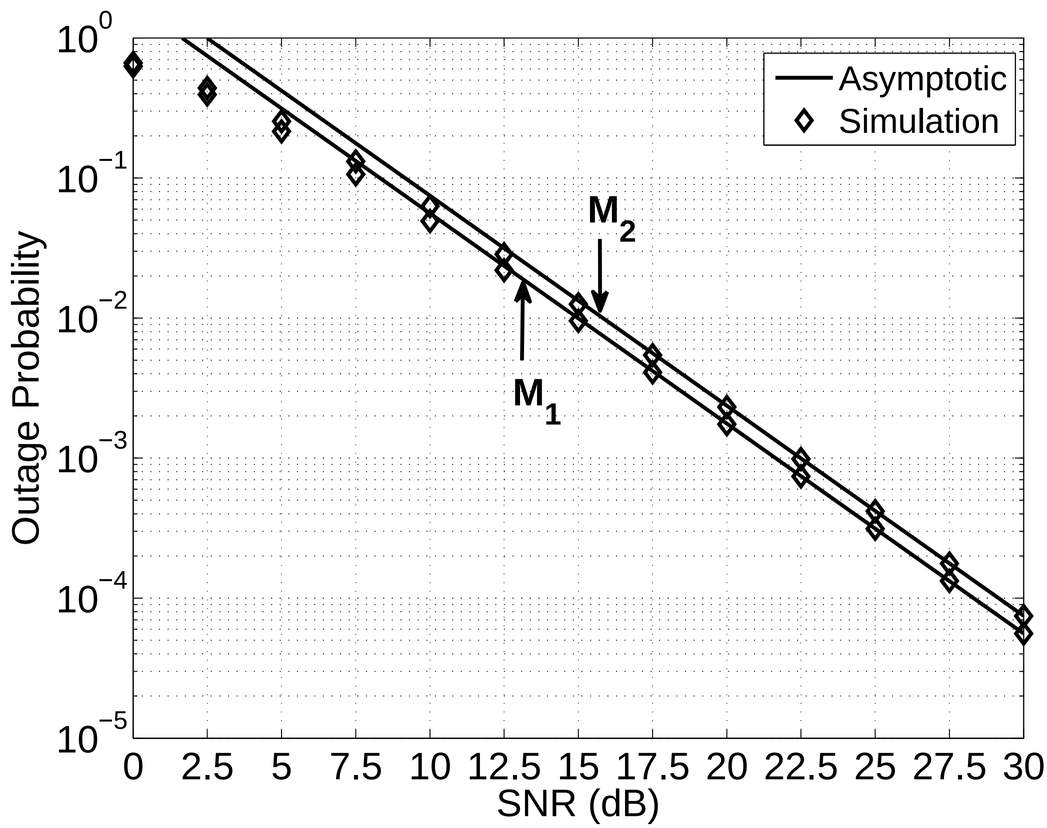

Figure 3.3: The asymptotic and simulated outage probabilities of SC over 3-branch correlated Nakagami-m channel with matrices $\mathbf{M}_1$ and $\mathbf{M}_2$ when $m = 0.5$.

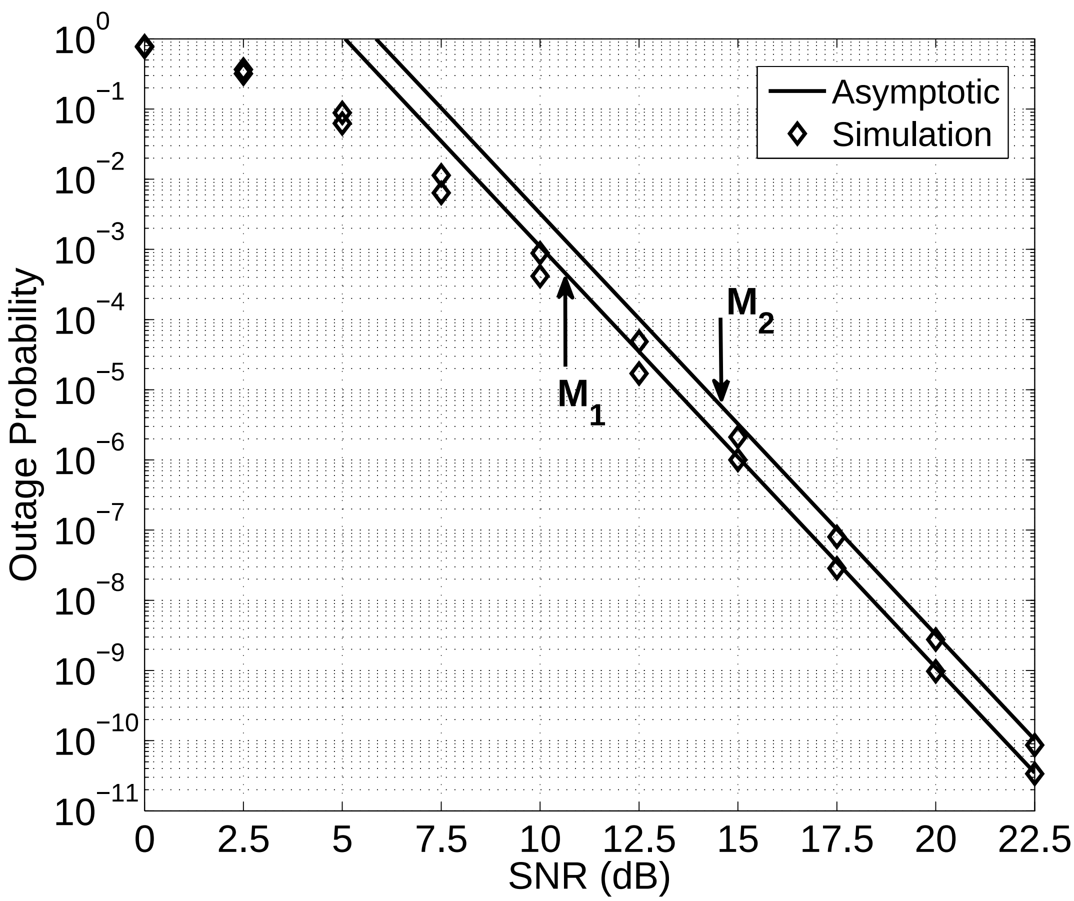

Figure 3.4: The asymptotic and simulated outage probabilities of SC over 3-branch correlated Nakagami-m channel with matrices $\mathbf{M}_1$ and $\mathbf{M}_2$ when $m = 2$.

Chapter 4

Asymptotic Performance Analysis of EGC over Arbitrarily Correlated Nakagami-*m* Fading Channels

In this chapter, using an integral representation for the joint PDF of multiple correlated Nakagami-m RVs obtained in Chapter 2, we derive the MGF of the square root of instantaneous SNR at the output of equal gain combiner and obtain the asymptotic average SER and outage probability of EGC over arbitrarily correlated Nakagami-m channels.

4.1 System Model

Assume that there are L available diversity branches experiencing frequency-nonselective and slow Nakagamim-m fading with fading parameter m taking the same positive integer value. Let H_i be the instantaneous channel fading amplitude on the i-th branch, E_S be the average symbol energy of the transmitted data symbol, and let N_0 be the PSD of complex AWGN in the i-th branch. The instantaneous SNR of the i-th diversity branch, γ_i, is defined as

$$\gamma_i = |H_i|^2 \frac{E_S}{N_0} \tag{4.1}$$

and the average SNR of the i-th diversity branch, Γ_i, is given by

$$\Gamma_i = \mathrm{E}\left[|H_i|^2\right] \frac{E_S}{N_0}. \tag{4.2}$$

Recall in Chapter 2 that for EGC, the instantaneous SNR at the output of the equal gain combiner is given by

$$\gamma_{EGC} = \frac{\left(\sum_{i=1}^{L} H_i\right)^2 E_S}{L N_0}. \tag{4.3}$$

4.2 MGF of Square Root of Instantaneous SNR at the Output of EGC

We now use the method described in Chapter 2 to construct correlated Nakagami-m RVs $H_1, H_2, \ldots, H_L$. Then the joint PDF of $H_1, H_2, \ldots, H_L$ can be expressed as (2.25). Let $\mathbf{R}$ denote the branch power covariance coefficient matrix whose (ik)-th element $(\mathbf{R})_{ik}$ is defined by (3.11). Define $\mathbf{M}$ as the matrix whose (ik)-th entry is given by (3.15), then the determinant of matrix $\mathbf{M}$ can be expressed as (3.16).

Using a series expansion of first kind modified Bessel function in [26, eq. (8.445)], when $x \to 0$, $I_{m-1}(x)$ can be written as

$$I_{m-1}(x) = \frac{1}{\Gamma(m)} \left(\frac{x}{2}\right)^{m-1} + o\left(x^{m-1}\right). \tag{4.4}$$

Define $H_E = \sqrt{\gamma_{EGC}}$. By (4.3), when $\gamma_{EGC} \to 0$, $H_i \to 0$. Substituting (4.4) into (2.25), we can write the joint PDF of $H_1, H_2, \cdots, H_L$ as

$$f(h_1, h_2, \cdots, h_L) = \frac{1}{\det^m(\mathbf{M})} \prod_{i=1}^{L} \frac{2}{\Gamma(m)} \frac{1}{\sigma_i^{2m}} \left[h_i^{2m-1} + o(h_i^{2m-1})\right] \exp\left[-\frac{h_i^2}{\sigma_i^2(1-\rho_i)}\right]. \tag{4.5}$$

Using (4.5), by definition, the MGF of H_E can be written as

$$\begin{aligned}\mathscr{M}_{H_E}(s) &= \mathrm{E}_{H_E}\left[e^{-sH_E}\right] \\ &= \mathrm{E}_{H_1,H_2,\cdots,H_L}\left[e^{-\frac{s(H_1+H_2+\cdots+H_L)\sqrt{E_S}}{\sqrt{LN_0}}}\right] \\ &= \frac{1}{\det^m(\mathbf{M})}\left[\frac{2}{\Gamma(m)}\right]^L \prod_{i=1}^{L} g_i(s)\end{aligned} \tag{4.6}$$

where $g_i(s)$ is given by

$$g_i(s) = \int_0^\infty \left(\frac{m\frac{E_S}{N_0}}{\Gamma_i}\right)^m \left[h_i^{2m-1} + o(h_i^{2m-1})\right] \exp\left[-\frac{h_i^2 m\frac{E_S}{N_0}}{\Gamma_i(1-\rho_i)}\right] \exp\left(-sh_i\sqrt{\frac{E_S}{LN_0}}\right) dh_i. \tag{4.7}$$

Using [26, eqs. (3.462) and (9.246)], we can show that when $s \to \infty$, $g_i(s)$ can be written as

$$g_i(s) = \Gamma(2m)\left(\frac{mL}{\Gamma_i}\right)^m \left[\frac{1}{s^{2m}} + o\left(\frac{1}{s^{2m}}\right)\right]. \tag{4.8}$$

Substituting (4.8) into (4.6), we obtain the MGF of H_E as

$$\mathscr{M}_{H_E}(s) = \frac{(mL)^{mL}}{\det^m(\mathbf{M})}\left[\frac{2\Gamma(2m)}{\Gamma(m)}\right]^L \frac{1}{\prod_{i=1}^L \Gamma_i^m}\left[\frac{1}{s^{2mL}} + o\left(\frac{1}{s^{2mL}}\right)\right]. \tag{4.9}$$

The MGF expression obtained in (4.9) will be used in studying the asymptotic error rate and outage probability of EGC.

4.3 Asymptotic Performance Analysis of EGC

Comparing (4.9) with (2.15) in Chapter 2, we observe that

$$t = mL - 1 \tag{4.10}$$

and

$$c = \frac{2^{L-1}}{\Gamma(2mL)} \left[\frac{\Gamma(2m)}{\Gamma(m)}\right]^L \frac{(mL)^{mL}}{\det^m(\mathbf{M})} \frac{\bar{\gamma}^{mL}}{\prod_{i=1}^{L} \Gamma_i^m}. \tag{4.11}$$

From (4.10), it is obvious that the diversity order G_d is mL.

4.3.1 Asymptotic Error Rate

The asymptotic SER of EGC reception with coherent modulation can be expressed from (2.11) as

$$P_e^E = \frac{[\Gamma(2m)]^L (mL)^{mL} p}{2^{mL+1-L}\Gamma(mL+1)[\Gamma(m)]^L \det^m(\mathbf{M})} \frac{1}{\prod_{i=1}^{L}(q\Gamma_i)^m} + o\left(\frac{1}{\prod_{i=1}^{L}\Gamma_i^m}\right). \tag{4.12}$$

In the special case of $m = 1$, it can be shown that (4.12) agrees with the asymptotic symbol error rate of EGC reception over arbitrarily correlated Rayleigh channels [5, eq. (5)].

4.3.2 Asymptotic Outage Probabilities

Substituting (4.10) and (4.11) into (3.26), we obtain the outage probability

$$P_{out}^E(\gamma_{th}) = \frac{2^{L-1}[\Gamma(2m)]^L (mL)^{mL-1}}{\Gamma(2mL)[\Gamma(m)]^L \det^m(\mathbf{M})} \frac{\gamma_{th}^{mL}}{\prod_{i=1}^{L}\Gamma_i^m} + o\left(\frac{1}{\prod_{i=1}^{L}\Gamma_i^m}\right). \tag{4.13}$$

When $m = 1$, it can be shown that (4.13) agrees with the asymptotic outage probability of EGC reception over arbitrarily correlated Rayleigh channels [5, eq. (13)].

Equations (4.12) and (4.13) are important new results. Although we deduce these results for integer fading parameter m, our numerical results suggest they are also valid at least for $m = 0.5$.

4.4 Discussions and Numerical Results

4.4.1 Discussions

Since $\det(\mathbf{M}) = 1$ for independent fading channels, we observe from (3.23) and (3.24) that the asymptotic SER of EGC over arbitrarily correlated Nakagami-*m* fading channels can be expressed in terms of the asymptotic SER over independent Nakagami-*m* fading channels scaled by a factor $\det^m(\mathbf{M})$, i.e.,

$$(P_e^{EGC})_{asym} = \frac{(P_{e,i}^{EGC})_{asym}}{\det^m(\mathbf{M})} \tag{4.14}$$

where $(P_{e,i}^{EGC})_{asym}$ denotes the asymptotic SER of EGC over independent Nakagami-*m* fading branches. In (4.14) the factor $\det^m(\mathbf{M})$ can be considered as the loss factor due to channel correlation. It should be noted that the simple relationship in (4.14) also holds for MRC over arbitrarily correlated Nakagami-*m* fading channels [25]. Finally a relationship similar to (4.14) can also be seen for the outage probability from (3.27).

4.4.2 Numerical Results

In this subsection, we present some numerical results of coherent BPSK with three-branch EGC over correlated Nakagami-*m* fading channels. We use the method proposed in [57] to generate correlated Nakagami RVs. For all the numerical results obtained here, we have assumed three-branch diversity reception with $\Gamma_1 = \Gamma_2 = \Gamma_3$ and $\gamma_{th} = 3$ dB. We use $\tilde{\rho} = [\boldsymbol{\rho_1}, \boldsymbol{\rho_2}, \boldsymbol{\rho_3}]$ to denote a vector whose elements comprise the power covariance coefficient matrix. For comparison, we set $\tilde{\boldsymbol{\rho}}_\mathbf{1} = [0.3968, 0.5265, 0.7861]$ and $\tilde{\boldsymbol{\rho}}_\mathbf{2} = [0.5008, 0.6229, 0.8264]$.

By (3.12) and (3.15), we obtain

$$\mathbf{M}_1 = \begin{pmatrix} 1 & 0.4571 & 0.5585 \\ 0.4571 & 1 & 0.6433 \\ 0.5585 & 0.6433 & 1 \end{pmatrix}$$

and

$$\mathbf{M}_2 = \begin{pmatrix} 1 & 0.5585 & 0.6433 \\ 0.5585 & 1 & 0.7175 \\ 0.6433 & 0.7175 & 1 \end{pmatrix}.$$

It follows that det($\mathbf{M}_1$)= 0.3937 and det($\mathbf{M}_2$)= 0.2750. From (4.14), the determinant inequality $\det(\mathbf{M}_1) > \det(\mathbf{M}_2)$ predicts that more highly correlated fading channels will lead to worse SER performance, as one expects. This is confirmed by the BER curves shown in Fig. 4.1 and Fig. 4.2 for $m = 0.5$ and $m = 2$ respectively. As seen from Fig. 4.1 and 4.2, the asymptotic error rates are accurate for SNR greater than 20 dB.

Fig. 4.3 and Fig. 4.4 plot the asymptotic and simulated outage probabilities of three-branch EGC with matrices $\mathbf{M}_1$ and $\mathbf{M}_2$ for $m = 0.5$ and $m = 2$ respectively. Figs. 4.1- 4.4 indicate that the analytical asymptotic results have excellent agreement with the simulated result in large SNR regions. This implies that the analytical asymptotic results can be used to predict small values of error rate and outage probability accurately for large SNR regions, where Monte Carlo simulation becomes time-consuming. Note that Fig. 4.1 and Fig. 4.3 also suggest that (4.12) and (4.13) are also valid at least for $m = 0.5$.

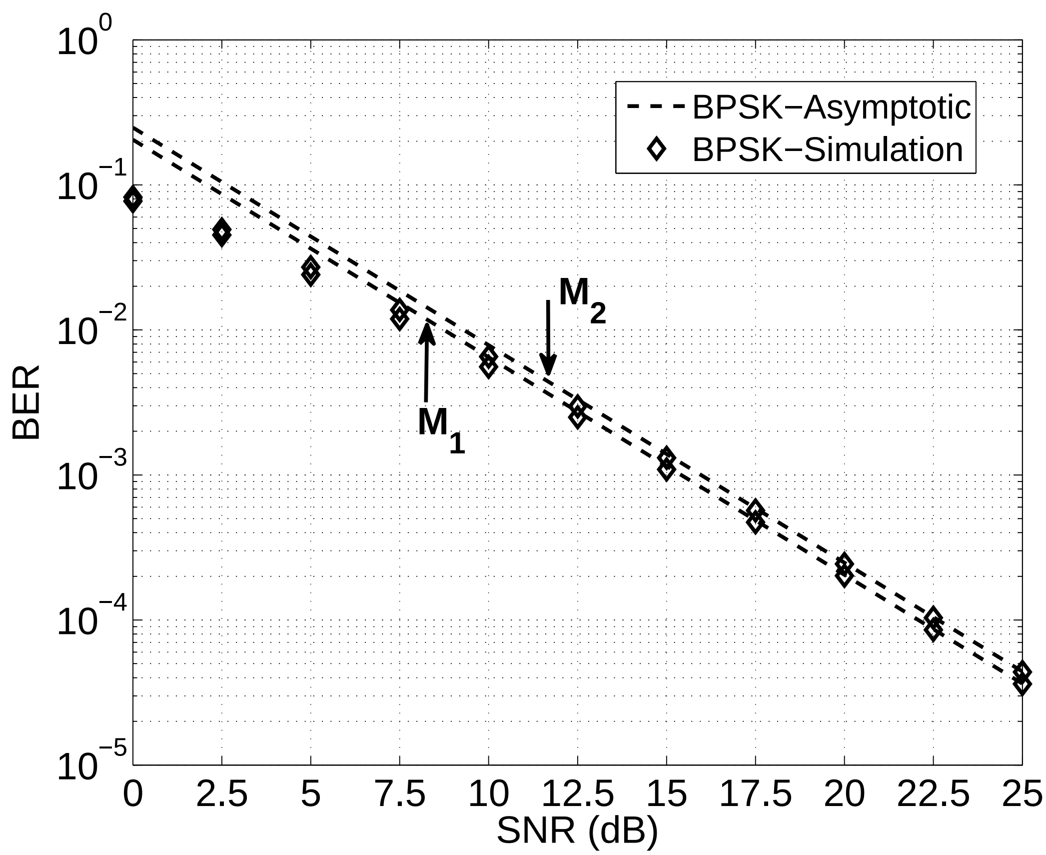

Figure 4.1: The asymptotic and simulated BERs of BPSK for EGC over 3-branch correlated Nakagami-m channels with matrices $\mathbf{M}_1$ and $\mathbf{M}_2$ when $m = 0.5$.

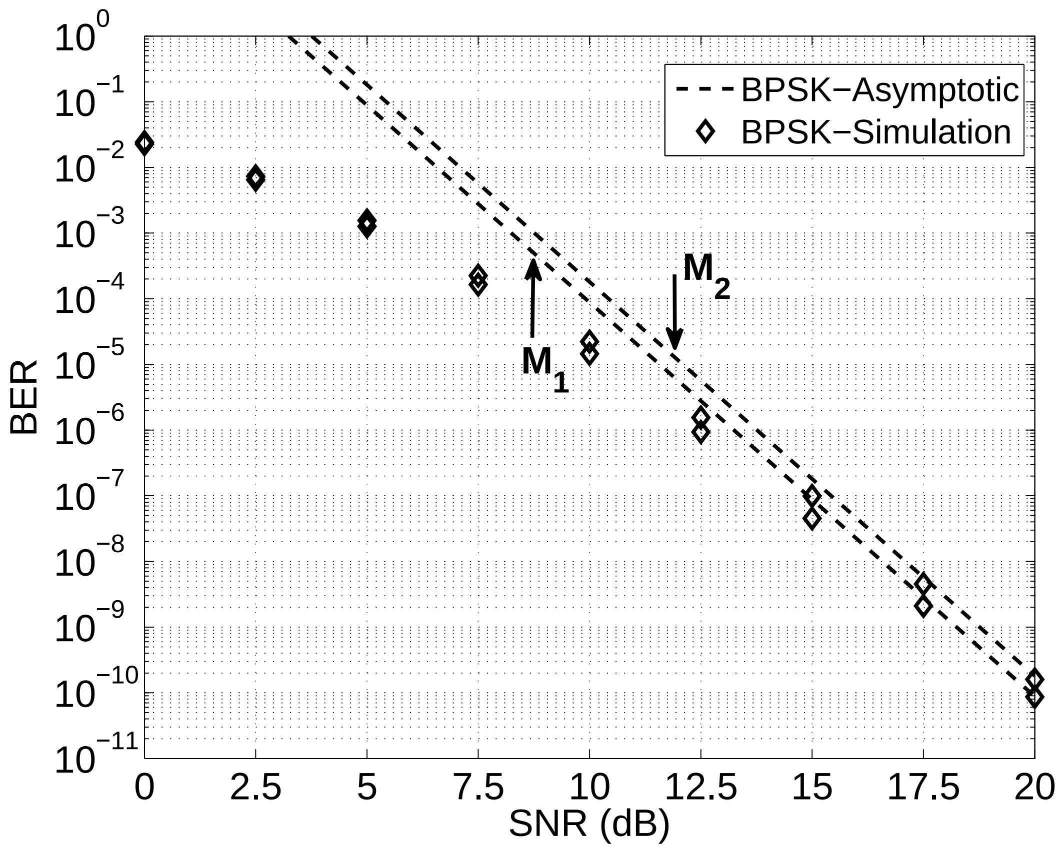

Figure 4.2: The asymptotic and simulated BERs of BPSK for EGC over 3-branch correlated Nakagami-m channels with matrices $\mathbf{M}_1$ and $\mathbf{M}_2$ when $m = 2$.

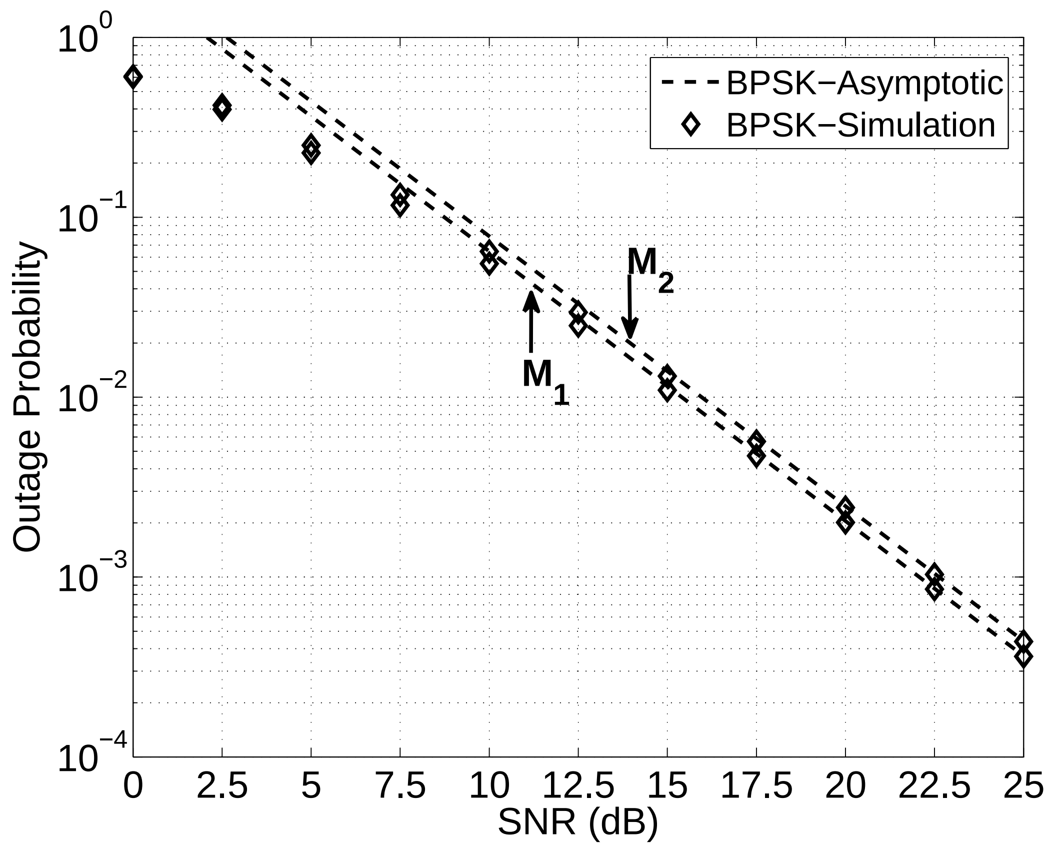

Figure 4.3: The asymptotic and simulated outage probabilities of EGC over 3-branch correlated Nakagami-m channel with matrices $\mathbf{M}_1$ and $\mathbf{M}_2$ when $m = 0.5$.

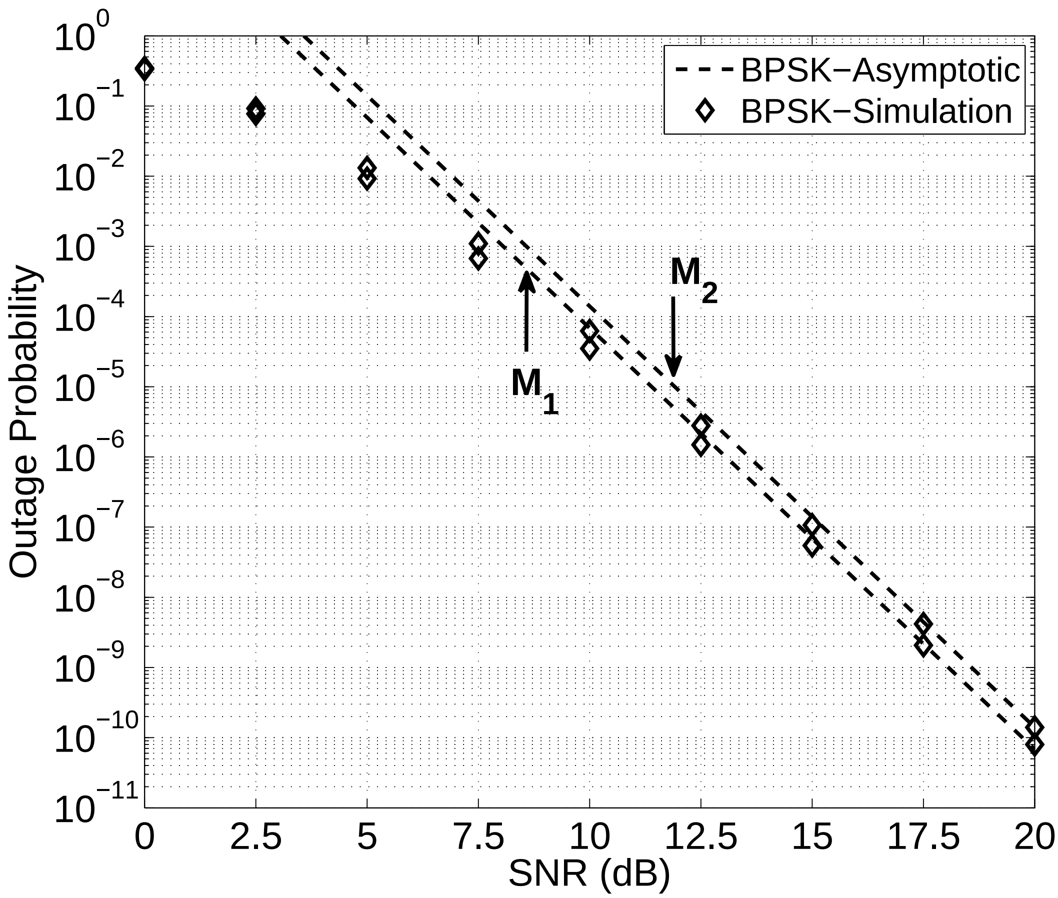

Figure 4.4: The asymptotic and simulated outage probabilities of EGC over 3-branch correlated Nakagami-m channel with matrices $\mathbf{M}_1$ and $\mathbf{M}_2$ when $m = 2$.

Chapter 5

Conclusions

In this chapter, we first summarize the contributions of this work, and then suggest some future work.

5.1 Summary of Contributions

This thesis makes the following contributions:

1. An asymptotic error rate expression for noncoherent modulation in large SNR regions has been derived. This expression can be used to estimate the high SNR SER or BER of various noncoherent modulation schemes, such as BNCFSK and BDPSK.

2. A new series representation of the generalized Marcum Q-function and a simple approximation for the Marcum Q-function $Q_m(\alpha, \beta)$ when $\beta \to 0^+$ have been derived. Numerical results show that the relative error between the exact value obtained by using the function NCX2CDF and the approximate value becomes small when $\beta \to 0^+$, and therefore the small argument approximation of the Marcum Q-function is highly accurate.

3. Closed-form error rate and outage probability expressions are derived for multi-branch EGC and SC over arbitrarily correlated Nakagami-m fading channels. They can be used to provide accurate and rapid estimation of error rates and outage probabilities in large SNR regions, where Monte Carlo simulation becomes time-consuming. These simple expressions will allow wireless system engineers to estimate the required fading

margin in link budget analysis without resorting to time-consuming computer simulations.

4. Simple relationships have been established for the asymptotic error rates and outage probabilities of EGC and SC over arbitrarily correlated and independent Nakagami-m fading channels. The same relationship also holds for MRC. It has been shown that the asymptotic error rate and outage probability over correlated branches can be obtained by scaling the asymptotic error rate and outage probability over independent branches with a factor, $\det^m(\mathbf{M})$, where $\det(\mathbf{M})$ is the determinant of matrix $\mathbf{M}$ whose elements are the square root of corresponding elements in the branch power covariance correlation matrix $\mathbf{R}$. The factor $\det^m(\mathbf{M})$ can be considered as the loss factor due to channel correlation. These significant relationships explain theoretically the observation that more highly correlated fading channels lead to worse error rate and outage probability performance.

5.2 Future Work

In this work, it is assumed that all the correlated Nakagami-m fading channels have the same integer-valued fading parameter m. However, the correlated Nakagami-m fading channels with different fading parameters can exist in some practical transmission scenarios. Because of the validity and feasibility of asymptotic techniques for large SNRs, the asymptotic technique can be extended to the study of the performance of multi-branch diversity combinings over correlated Nakagami-m fading channels with arbitrarily-valued fading parameters.

In addition, so far there exists no method that can accurately generate multiple correlated Nakagami-m RVs with arbitrary fading parameters and mean square values. In [57], Zhang proposed a decomposition technique to generate multiple correlated Nakagami-m RVs with same fading parameters. Zhang's algorithm is inaccurate when $2m$ is not an integer. In our future research, we will develop an accurate method to generate multiple correlated

Nakagami-m RVs with arbitrary fading parameters and mean square values.

Bibliography

[1] L. Anderson, *Nikola Tesla on His Work With Alternating Currents and Their Application to Wireless Telegraphy, Telephony, and Transmission of Power: An Extended Interview*. Breckenridge, Colo: Twenty-First Century Books, 2002.

[2] M. K. Simon and M. S. Alouini, *Digital Communication Over Fading Channels*, 2nd ed. New York: Wiley-IEEE Press, 2004.

[3] G. L. Stüber, *Principles of Mobile Communications*. Norwell, MA: Kluwer, 1996.

[4] L. Shuo, "Asymptotic analysis of multi-branch combining techniques over arbitrarily correlated fading channels," M.Sc. thesis, University of Alberta, Edmonton, Alberta, 2008.

[5] S. Liu, J. Cheng, and N. C. Beaulieu, "Asymptotic error analysis of diversity schemes on arbitrarily correlated Rayleigh fading channels," *IEEE Transactions on Communications*, vol. 58, pp. 1351–1355, May 2010.

[6] A. Bajwa, "UHF wideband statistical model and simulation of mobile radio multipath propagation effects," in *Proc. IEE Communications, Radar and Signal Processing*, Aug. 1985, vol. 132, pp. 327–333.

[7] F. Patenaude, J. Lodge, and J.-Y. Chouinard, "Eigen-analysis of wideband fading channel impulse responses," *IEEE Transactions on Vehicular Technology*, vol. 48, pp. 593–606, Mar. 1999.

[8] M. K. Simon and M.-S. Alouini, "A unified performance analysis of digital communication with dual selective combining diversity over correlated Rayleigh and Nakagami-*m* fading channels," *IEEE Transactions on Communications*, vol. 47, pp. 33–44, Jan. 1999.

[9] Y.-C. Ko, M.-S. Alouini, and M. K. Simon, "Average SNR of dual selection combining over correlated Nakagami-*m* fading channels," *IEEE Communications Letters*, vol. 4, pp. 12–14, Jan. 2000.

[10] C. Tellambura, A. Annamalai, and V. K. Bhargava, "Closed-form and infinite series solutions for the MGF of a dual-diversity selection combining output in bivariate Nakagami fading," *IEEE Communications Letters*, vol. 51, pp. 539–542, Apr. 2003.

[11] G. K. Karagiannidis, D. A. Zogas, and S. A. Kotsopoulos, "Performance analysis of triple selection diversity over exponentially correlated Nakagami-*m* fading channels," *IEEE Transactions on Communications*, vol. 51, pp. 1245–1248, Aug. 2003.

[12] D. A. Zogas, G. K. Karagiannidis, and S. A. Kotsopoulos, "On the average output SNR in selection combining with three correlated branches over Nakagami-*m* fading channels," *IEEE Transactions on Wireless Communications*, vol. 3, pp. 25–28, Jan. 2004.

[13] Q. T. Zhang and H. G. Lu, "A general analytical approach to multibranch selection combining over various spatially correlated fading channels," *IEEE Transactions on Communications*, vol. 50, pp. 1066–1073, July 2002.

[14] X. Zhang and N. C. Beaulieu, "Performance analysis of generalized selection combining in generalized correlated Nakagami-*m* fading," *IEEE Transactions on Communications*, vol. 54, pp. 2103–2112, Nov. 2006.

[15] G. K. Karagiannidis, D. A. Zogas, and S. A. Kotsopoulos, "On the multivariate

Nakagami-*m* distribution with exponential correlation," *IEEE Transactions on Communications*, vol. 51, pp. 1240–1244, Aug. 2003.

[16] G. K. Karagiannidis, D. A. Zogas, and S. A. Kotsopoulos, "An efficient approach to multivariate Nakagami-*m* distribution using Green's matrix approximation," *IEEE Transactions on Wireless Communications*, vol. 2, pp. 883–889, Sept. 2003.

[17] Y. Chen and C. Tellambura, "Distribution functions of selection combiner output in equally correlated Rayleigh, Rician, and Nakagami-*m* fading channels," *IEEE Transactions on Communications*, vol. 52, pp. 1948–1956, Nov. 2004.

[18] Y. Chen and C. Tellambura, "Moment analysis of the equal gain combiner output in equally correlated fading channels," *IEEE Transactions on Vehicular Technology*, vol. 54, pp. 1971–1979, Nov. 2005.

[19] G. K. Karagiannidis, "Moments-based approach to the performance analysis of equal gain diversity in Nakagami-*m* fading," *IEEE Transactions on Communications*, vol. 52, pp. 685–690, May 2004.

[20] J. Hu and N. C. Beaulieu, "Accurate closed-form approximations for the performance of equal gain combining diversity systems in Nakagami fading channels," *European Transactions on Telecommunications*, vol. 19, pp. 707–717, 2008.

[21] D. B. da Costa, M. D. Yacoub, and J. Santos Filho, "An improved closed-form approximation to the sum of arbitrary Nakagami-*m* variates," *IEEE Transactions on Vehicular Technology*, vol. 57, pp. 3854–3858, Nov. 2008.

[22] Z. Hadzi-Velkov, N. Zlatanov, and G. K. Karagiannidis, "An accurate approximation to the distribution of the sum of equally correlated Nakagami-*m* envelopes and its application in equal gain diversity receivers," in *Proc. IEEE International Conference on Communications, ICC 2009*, Dresden, Germany, June 14–18 2009, pp. 1–5.

[23] N. Zlatanov, Z. Hadzi-Velkov, and G. K. Karagiannidis, "An efficient approximation to the correlated Nakagami-m sums and its application in equal gain diversity receivers," *IEEE Transactions on Wireless Communications*, vol. 9, pp. 302–310, Jan. 2010.

[24] H. S. Abdel-Ghaffar and S. Pasupathy, "Asymptotic performance of M-ary and binary signals over multipath/multichannel Rayleigh and Rician fading," *IEEE Transactions on Communications*, vol. 43, pp. 2721–2731, Nov. 1995.

[25] Z. Wang and G. B. Giannakis, "A simple and general parameterization quantifying performance in fading channels," *IEEE Transactions on Communications*, vol. 51, pp. 1389–1398, Aug. 2003.

[26] I. S. Gradshteyn and I. M. Ryzhik, *Table of Integrals, Series, and Products*, 6th ed. San Diego: Academic Press, 2000.

[27] M. Nakagami, "The m-distribution, a general formula of intensity distribution of rapid fading," *Statistical Methods in Radio Wave Propagation*, vol. 40, pp. 757–768, Nov. 1962.

[28] D. G. Brennan, "Linear diversity combining techniques," in *Proc. IRE*, June 1959, vol. 47, pp. 1057–1102.

[29] J. G. Proakis, *Digital Communications*, 3rd ed. New York: McGraw-Hill, 1995.

[30] Y. L. Tong, *The Multivariate Normal Distribution*. New York: Spring-Verlag, 1990.

[31] M. Abramowitz and I. A. Stegun, Eds., *Handbook of Mathematical Functions*, 10th ed. New York: Dover Publications, 1972.

[32] J. I. Marcum, "A statistical theory of target detection by pulsed radar," *IRE Transactions on Information Theory*, vol. 6, pp. 59–267, Apr. 1960.

[33] A. H. M. Ross, "Algorithms for calculating the noncentral chi-square distribution," *IEEE Transactions on Information Theory*, vol. 45, pp. 1327–1333, May 1999.

[34] C. W. Helstrom, "Computing the generalized Marcum Q-function," *IEEE Transactions on Information Theory*, vol. 38, pp. 1422–1428, July 1992.

[35] G. H. Robertson, "Computation of the noncentral chi-square distribution," *Bell System Technical Journal*, vol. 48, pp. 201–207, Jan. 1969.

[36] G. M. Dillard, "Recursive computation of the generalized Q function," *IEEE Transactions on Aerospace and Electronic Systems*, vol. 9, pp. 614–615, July 1973.

[37] D. A. Shnidman, "Efficient evaluation of probabilities of detection and the generalized Q-function," *IEEE Transactions on Information Theory*, vol. 22, pp. 746–759, Nov. 1976.

[38] S. Parl, "A new method of calculating the generalized Q function," *IEEE Transactions on Information Theory*, vol. 26, pp. 121–124, Jan. 1980.

[39] C. Tellambura, A. Annamalai, and V. K. Bhargava, "Contour integral representation for generalized Marcum Q-function and its application to unified analysis of dual-branch selection diversity over correlated Nakagami-m fading channels," in *Proc. IEEE Vehicular Technology Conference, VTC 2000*, Tokyo, Japan, May 15–18 2000, vol. 2, pp. 1031–1034.

[40] M. K. Simon and M.-S. Alouini, "Some new results for integrals involving the generalized Marcum Q-function and their application to performance evaluation over fading channels," *IEEE Transactions on Wireless Communications*, vol. 2, pp. 611–615, July 2003.

[41] G. Weinberg, "Poisson representation and monte carlo estimation of generalized Marcum Q-function," *IEEE Transactions on Aerospace and Electronic Systems*, vol. 42, pp. 1520–1531, Oct. 2006.

[42] A. Annamalai and C. Tellambura, "A simple exponential integral representation of the generalized Marcum Q-function $Q_M(a,b)$ for real-order Q with applications," in *Proc. IEEE Military Communications Conference MILCOM 2008*, San Diego, CA, USA, Nov. 17–19 2008, pp. 1–7.

[43] A. Annamalai, C. Tellambura, and J. Matyjas, "A new twist on the generalized Marcum Q-function $Q_M(a,b)$ with fractional-order Q and its applications," in *Proc. IEEE Consumer Communications and Networking Conference CCNC 2009*, Las Vegas, NV, USA, Jan. 11–13 2009, pp. 1–5.

[44] R. Li, P. Y. Kam, and H. Fu, "New representations and bounds for the generalized Marcum Q-function via a geometric approach, and an application," *IEEE Transactions on Communications*, vol. 58, pp. 157–169, Jan. 2010.

[45] H. Fu, P. Y. Kam, and R. Li, "Geometric-view-based evaluation of generalized Marcum Q-function," in *Proc. IEEE Vehicular Technology Conference, VTC 2010*, Taipei, Taiwan, May 16–19 2010, pp. 1–5.

[46] M. K. Simon and M.-S. Alouini, "Exponential-type bounds on the generalized Marcum Q-function with application to error probability analysis over fading channels," *IEEE Transactions on Communications*, vol. 48, pp. 359–366, May 2000.

[47] A. Annamalai and C. Tellambura, "Cauchy-schwarz bound on the generalized Marcum Q-function with applications," *Wireless Communication and Mobile Computing*, vol. 1, pp. 243–253, Mar. 2001.

[48] R. Li and P. Y. Kam, "Computing and bounding the generalized Marcum Q-function via a geometric approach," in *Proc. IEEE International Symposium on Information Theory, ISIT 2006*, Seattle, WA, USA, July 9–14 2006, pp. 1090–1094.

[49] R. Li and P. Y. Kam, "Generic exponential bounds on the generalized Marcum Q-

function via the geometric approach," in *Proc. IEEE Globe Communications Conference, GLOBECOM 2007*, Washington, DC, USA, Nov. 25–30 2007, pp. 1754–1758.

[50] Y. Sun and S. Zhou, "Tight bounds of the generalized Marcum Q-function based on log-concavity," in *Proc. IEEE Globe Communications Conference, GLOBECOM 2008*, New Orleans, LA, USA, Dec. 1–5 2008, pp. 1–5.

[51] Z. Zhao, D. Gong, and Y. Li, "Tight geometric bound for Marcum Q-function," *IET Electronics Letters*, vol. 44, pp. 340–341, Feb. 2008.

[52] N. Ding and H. Zhang, "A flexible method to approximate Marcum Q-function based on geometric way of thinking," in *Proc. International Symposium on Communications, Control and Signal Processing, ISCCSP 2008*, Saint Julians, Malta, Mar. 12–14 2008, pp. 1351–1356.

[53] A. Baricz and Y. Sun, "New bounds for the generalized Marcum Q-function," *IEEE Transactions on Information Theory*, vol. 55, pp. 3091–3100, July 2009.

[54] A. Baricz, "Tight bounds for the generalized Marcum Q-function," *Journal of Mathematical Analysis and Applications*, vol. 360, pp. 265–277, Dec. 2009.

[55] Y. Sun, A. Baricz, and S. Zhou, "On the monotonicity, log-concavity and tight bounds of the generalized Marcum and Nuttall Q-functions," *IEEE Transactions on Information Theory*, vol. 56, pp. 1166–1186, Mar. 2010.

[56] C. D. Meyer, *Matrix Analysis and Applied Linear Algebra*. Philadelphia, PA: Society for Industrial and Applied Mathematics, 2000.

[57] Q. Zhang, "A decomposition technique for efficient generation of correlated Nakagami fading channels," *IEEE Journal on Selected Areas in Communications*, vol. 18, pp. 2385–2392, Nov. 2000.

Appendix A

Derivation of Error Rate for Noncoherent Modulation

Let A be a small fixed positive number such that when $\beta < A$, the PDF of β can be written as $f(\beta) = c\beta^t + o(\beta^t)$. Then the average SER for noncoherent modulation with conditional SER $p_e(\beta) = p\exp(-q\beta\bar{\gamma})$ can be caculated as

$$\begin{aligned}
P_e &= \int_0^\infty p_e(\beta) f(\beta) d\beta \\
&= \int_0^\infty p\exp(-q\beta\bar{\gamma}) f(\beta) d\beta \\
&= p\int_0^A \exp(-q\beta\bar{\gamma}) f(\beta) d\beta + p\int_A^\infty \exp(-q\beta\bar{\gamma}) f(\beta) d\beta \\
&= p\int_0^\infty \int_{q\beta\bar{\gamma}}^\infty \exp(-x)\left[c\beta^t + o\left(\beta^t\right)\right] dx d\beta \\
&\quad - p\int_A^\infty \int_{q\beta\bar{\gamma}}^\infty \exp(-x)\left[c\beta^t + o\left(\beta^t\right)\right] dx d\beta \\
&\quad + p\int_A^\infty \exp(-q\beta\bar{\gamma}) f(\beta) d\beta
\end{aligned} \tag{A.1}$$

where in obtaining the last equality we have used a fact $e^{-x} = \int_x^\infty e^{-y} dy$. The first integral in (A.1) can be written as

$$\begin{aligned}
& p \int_0^\infty \int_{q\beta\bar{\gamma}}^\infty \exp(-x) \left[c\beta^t + o\left(\beta^t\right)\right] dx d\beta \\
&= cp \int_0^\infty \int_{q\beta\bar{\gamma}}^\infty \exp(-x) \beta^t dx d\beta + p \int_0^\infty \exp\left(-q\beta\bar{\gamma}\right) o\left(\beta^t\right) d\beta \\
&= cp \int_0^\infty \left[\int_0^{\frac{x}{q\bar{\gamma}}} \beta^t d\beta\right] \exp\left(-x\right) dx + o\left(\bar{\gamma}^{-(t+1)}\right) \\
&= \frac{cp}{(t+1)\left(q\bar{\gamma}\right)^{t+1}} \int_0^\infty x^{t+1} \exp\left(-x\right) dx + o\left(\bar{\gamma}^{-(t+1)}\right) \\
&= \frac{c\Gamma\left(t+2\right) p}{(t+1)\left(q\bar{\gamma}\right)^{t+1}} + o\left(\bar{\gamma}^{-(t+1)}\right). \qquad \text{(A.2)}
\end{aligned}$$

Ignoring the term $o\left(\beta^t\right)$, the second integral in (A.1) can be expressed as

$$\begin{aligned}
& cp \int_A^\infty \int_{q\beta\bar{\gamma}}^\infty \exp(-x) \beta^t dx d\beta \\
&= cp \int_{Aq\bar{\gamma}}^\infty \left[\int_A^{\frac{x}{q\bar{\gamma}}} \beta^t d\beta\right] \exp\left(-x\right) dx \\
&= cp \int_{Aq\bar{\gamma}}^\infty \left[\frac{\beta^{t+1}}{t+1}\right]_A^{\frac{x}{q\bar{\gamma}}} \exp\left(-x\right) dx \\
&= \frac{cp}{(t+1)\left(q\bar{\gamma}\right)^{t+1}} \int_{Aq\bar{\gamma}}^\infty \exp\left(-x\right) \left[x^{t+1} - \left(Aq\bar{\gamma}\right)^{t+1}\right] dx. \qquad \text{(A.3)}
\end{aligned}$$

The integral in (A.3) becomes zero as $\bar{\gamma} \to \infty$. Therefore, the second integral can be written as $o\left(\bar{\gamma}^{-(t+1)}\right)$.

For the third integral in (A.1) we have the following relation

$$\begin{aligned}
p \int_A^\infty \exp(-q\beta\bar{\gamma}) f(\beta) d\beta &\leq p \int_A^\infty \exp\left(-qA\bar{\gamma}\right) f\left(\beta\right) d\beta \\
&= p \cdot \exp\left(-qA\bar{\gamma}\right) \int_A^\infty f\left(\beta\right) d\beta \\
&\leq p \cdot \exp\left(-qA\bar{\gamma}\right) \qquad \text{(A.4)}
\end{aligned}$$

and

$$\lim_{\bar{\gamma}\to\infty} \frac{\exp\left(-qA\bar{\gamma}\right)}{\bar{\gamma}^{-(t+1)}} = \lim_{\bar{\gamma}\to\infty} \frac{\bar{\gamma}^{t+1}}{\exp\left(qA\bar{\gamma}\right)} = 0. \tag{A.5}$$

Therefore, the third integral can be written as $o\left(\bar{\gamma}^{-(t+1)}\right)$.

Finally, it follows that the average SER for noncoherent modulation at large SNR can be expressed as (2.12).

Appendix B

Derivation of (2.18)

According to (2.17), for $i \in \{1, \cdots, L\}$ and $l, p \in \{1, \cdots, m\}, l \neq p$, we have the following expressions

$$\begin{aligned} |G_{il}|^2 = \sigma_i^2 &\left[(1-\rho_i) X_{il}^2 + \rho_i X_{0l}^2 + 2\sqrt{\rho_i(1-\rho_i)} X_{il} X_{0l} \right] \\ + \sigma_i^2 &\left[(1-\rho_i) Y_{il}^2 + \rho_i Y_{0l}^2 + 2\sqrt{\rho_i(1-\rho_i)} Y_{il} Y_{0l} \right] \end{aligned} \tag{B.1}$$

and

$$\begin{aligned} \frac{|G_{il}|^4}{\sigma_i^4} =\ & (1-\rho_i)^2 X_{il}^4 + \rho_i^2 X_{0l}^4 + 4\rho_i(1-\rho_i) X_{il}^2 X_{0l}^2 + (1-\rho_i)^2 Y_{il}^4 + \rho_i^2 Y_{0l}^4 \\ & + 4\rho_i(1-\rho_i) Y_{il}^2 Y_{0l}^2 + 2\rho_i(1-\rho_i) X_{il}^2 X_{0l}^2 + 4(1-\rho_i)\sqrt{\rho_i(1-\rho_i)} X_{il}^3 X_{0l} \\ & + 2(1-\rho_i)^2 X_{il}^2 Y_{il}^2 + 2\rho_i(1-\rho_i) X_{il}^2 Y_{0l}^2 + 4(1-\rho_i)\sqrt{\rho_i(1-\rho_i)} X_{il}^2 Y_{il} Y_{0l} \\ & + 4\rho_i\sqrt{\rho_i(1-\rho_i)} X_{0l}^3 X_{il} + 2\rho_i(1-\rho_i) X_{0l}^2 Y_{il}^2 + 2\rho_i^2 X_{0l}^2 Y_{0l}^2 \\ & + 4\rho_i\sqrt{\rho_i(1-\rho_i)} X_{0l}^2 Y_{il} Y_{0l} + 4(1-\rho_i)\sqrt{\rho_i(1-\rho_i)} X_{il} X_{0l} Y_{il}^2 \\ & + 4\rho_i\sqrt{\rho_i(1-\rho_i)} X_{il} X_{0l} Y_{0l}^2 + 8\rho_i(1-\rho_i) X_{il} X_{0l} Y_{il} Y_{0l} + 2\rho_i(1-\rho_i) Y_{il}^2 Y_{0l}^2 \\ & + 4(1-\rho_i)\sqrt{\rho_i(1-\rho_i)} Y_{il}^3 Y_{0l} + 4\rho_i\sqrt{\rho_i(1-\rho_i)} Y_{il} Y_{0l}^3 \end{aligned} \tag{B.2}$$

and

$$\begin{aligned}
\frac{|G_{il}|^2|G_{ip}|^2}{\sigma_i^4} = {} & (1-\rho_i)^2 X_{il}^2 X_{ip}^2 + \rho_i(1-\rho_i) X_{il}^2 X_{0p}^2 + 2(1-\rho_i)\sqrt{\rho_i(1-\rho_i)} X_{il}^2 X_{ip} X_{0p} \\
& + (1-\rho_i)^2 X_{il}^2 Y_{ip}^2 + \rho_i(1-\rho_i) X_{il}^2 Y_{0p}^2 + 2(1-\rho_i)\sqrt{\rho_i(1-\rho_i)} X_{il}^2 Y_{ip} Y_{0p} \\
& + \rho_i(1-\rho_i) X_{0l}^2 X_{ip}^2 + \rho_i^2 X_{0l}^2 X_{0p}^2 + 2\rho_i\sqrt{\rho_i(1-\rho_i)} X_{0l}^2 X_{ip} X_{0p} \\
& + \rho_i(1-\rho_i) X_{0l}^2 Y_{ip}^2 + \rho_i^2 X_{0l}^2 Y_{0p}^2 + 2\rho_i\sqrt{\rho_i(1-\rho_i)} X_{0l}^2 Y_{ip} Y_{0p} \\
& + 2(1-\rho_i)\sqrt{\rho_i(1-\rho_i)} X_{il} X_{0l} X_{ip}^2 + 2\rho_i\sqrt{\rho_i(1-\rho_i)} X_{il} X_{0l} X_{0p}^2 \\
& + 4\rho_i(1-\rho_i) X_{il} X_{0l} X_{ip} X_{0p} + 2(1-\rho_i)\sqrt{\rho_i(1-\rho_i)} X_{il} X_{0l} Y_{ip}^2 \\
& + 2\rho_i\sqrt{\rho_i(1-\rho_i)} X_{il} X_{0l} Y_{0p}^2 + 4\rho_i(1-\rho_i) X_{il} X_{0l} Y_{ip} Y_{0p} \\
& + (1-\rho_i)^2 Y_{il}^2 X_{ip}^2 + \rho_i(1-\rho_i) Y_{il}^2 X_{0p}^2 + 2(1-\rho_i)\sqrt{\rho_i(1-\rho_i)} Y_{il}^2 X_{ip} X_{0p} \\
& + (1-\rho_i)^2 Y_{il}^2 Y_{ip}^2 + \rho_i(1-\rho_i) Y_{il}^2 Y_{0p}^2 + 2(1-\rho_i)\sqrt{\rho_i(1-\rho_i)} Y_{il}^2 Y_{ip} Y_{0p} \\
& + \rho_i(1-\rho_i) Y_{0l}^2 X_{ip}^2 + \rho_i^2 Y_{0l}^2 X_{0p}^2 + 2\rho_i\sqrt{\rho_i(1-\rho_i)} Y_{0l}^2 X_{ip} X_{0p} \\
& + \rho_i(1-\rho_i) Y_{0l}^2 Y_{ip}^2 + \rho_i^2 Y_{0l}^2 Y_{0p}^2 + 2\rho_i\sqrt{\rho_i(1-\rho_i)} Y_{0l}^2 Y_{ip} Y_{0p} \\
& + 2(1-\rho_i)\sqrt{\rho_i(1-\rho_i)} Y_{il} Y_{0l} X_{ip}^2 + 2\rho_i\sqrt{\rho_i(1-\rho_i)} Y_{il} Y_{0l} X_{0p}^2 \\
& + 4\rho_i(1-\rho_i) Y_{il} Y_{0l} X_{ip} X_{0p} + 2(1-\rho_i)\sqrt{\rho_i(1-\rho_i)} Y_{il} Y_{0l} Y_{ip}^2 \\
& + 2\rho_i\sqrt{\rho_i(1-\rho_i)} Y_{il} Y_{0l} Y_{0p}^2 + 4\rho_i(1-\rho_i) Y_{il} Y_{0l} Y_{ip} Y_{0p}. \qquad \text{(B.3)}
\end{aligned}$$

For any $u \in \{0,1,\cdots,L\}$, and $l \in \{1,\cdots,m\}$, X_{ul} and Y_{ul} are independent Gaussian RVs with distribution $\mathcal{N}(0,1/2)$, hence we have $\mathrm{E}[X_{ul}] = \mathrm{E}[Y_{ul}] = 0$, $\mathrm{E}\left[X_{ul}^2\right] = \mathrm{E}\left[Y_{ul}^2\right] = \frac{1}{2}$, $\mathrm{E}\left[X_{ul}^3\right] = \mathrm{E}\left[Y_{ul}^3\right] = 0$, and $\mathrm{E}\left[X_{ul}^4\right] = \mathrm{E}\left[Y_{ul}^4\right] = \frac{3}{4}$. Taking the expectation with respect to (B.2), (B.2), and (B.3), we can obtain $\mathrm{E}\left[|G_{il}|^2\right] = \sigma_i^2$, $\mathrm{E}\left[|G_{il}|^4\right] = 2\sigma_i^4$, and $\mathrm{E}\left[|G_{il}|^2|G_{ip}|^2\right] = \sigma_i^4$.

Since $R_i = \sum_{l=1}^m |G_{il}|^2$ and $R_k = \sum_{l=1}^m |G_{kl}|^2$, it follows that $\mathrm{E}[R_i] = m\sigma_i^2$ and

$\mathrm{E}[R_k] = m\sigma_k^2$. The mean square of R_i can be calculated as

$$\mathrm{E}\left[R_i^2\right] = \mathrm{E}\left[\left(\sum_{l=1}^{m}|G_{il}|^2\right)^2\right] = \sum_{l=1}^{m}\mathrm{E}\left[|G_{il}|^4\right] + \sum_{l=1}^{m}\sum_{\substack{p\neq l\\ p=1}}^{m}\mathrm{E}\left[|G_{il}|^2|G_{ip}|^2\right] = m(m+1)\sigma_i^4 \tag{B.4}$$

and the variance of R_i is given by

$$\mathrm{Var}[R_i] = \mathrm{E}\left[R_i^2\right] - \mathrm{E}[R_i]^2 = m\sigma_i^4. \tag{B.5}$$

Similarly, we have $\mathrm{Var}[R_k] = m\sigma_k^4$.

According to the definition of R_i and R_k, we have

$$R_iR_k = \sum_{l=1}^{m}\sum_{p=1}^{m}|G_{il}|^2|G_{kp}|^2. \tag{B.6}$$

Since X_{il}, X_{0l}, Y_{il}, and Y_{0l} are independent zero mean Gaussian RVs, we can ignore them when calculating $\mathrm{E}[R_iR_k]$. By symmetry, we can obtain

$$\begin{aligned}
\mathrm{E}[R_iR_k] &= 2\sigma_i^2\sigma_k^2\sum_{l=1}^{m}\sum_{p=1}^{m}\mathrm{E}\left[(1-\rho_i)X_{il}^2\left[(1-\rho_k)X_{kp}^2+\rho_kX_{0p}^2+(1-\rho_k)Y_{kp}^2+\rho_kY_{0p}^2\right]\right]\\
&\quad + 2\sigma_i^2\sigma_k^2\sum_{l=1}^{m}\sum_{\substack{p\neq l\\ p=1}}^{m}\mathrm{E}\left[\rho_iX_{0l}^2\left[(1-\rho_k)X_{kp}^2+\rho_kX_{0p}^2+(1-\rho_k)Y_{kp}^2+\rho_kY_{0p}^2\right]\right]\\
&\quad + 2\sigma_i^2\sigma_k^2\sum_{l=1}^{m}\mathrm{E}\left[\rho_iX_{0l}^2\left[(1-\rho_k)X_{kl}^2+\rho_kX_{0l}^2+(1-\rho_k)Y_{kl}^2+\rho_kY_{0l}^2\right]\right]\\
&= 2\sigma_i^2\sigma_k^2\left[\sum_{l=1}^{m}\sum_{p=1}^{m}\frac{1-\rho_i}{2}+2\sigma_i^2\sigma_k^2\sum_{l=1}^{m}\sum_{\substack{p\neq l\\ p=1}}^{m}\frac{\rho_i}{2}+2\sigma_i^2\sigma_k^2\sum_{l=1}^{m}\frac{\rho_i+\rho_k}{2}\right]\\
&= \sigma_i^2\sigma_k^2\left(m^2+m\rho_i\rho_k\right).
\end{aligned} \tag{B.7}$$

Noting that $\mathrm{E}[R_iR_k] = \sigma_i^2\sigma_k^2\left(m^2+m\rho_i\rho_k\right)$, $\mathrm{E}[R_i] = m\sigma_i^2$, $\mathrm{E}[R_k] = m\sigma_k^2$, $\mathrm{Var}[R_i] = m\sigma_i^4$, and

$\mathrm{Var}[R_k] = m\sigma_k^4$, by the definition of cross-correlation of R_i and R_k, we can finally obtain (2.18).

Appendix C

Derivation of (2.25)

Using variable transformation, we have

$$f(h_1, h_2, \cdots, h_L) = f(r_1, r_2, \cdots, r_L) \cdot |J(h_1, h_2, \cdots, h_L)| \tag{C.1}$$

where $|\cdot|$ is the absolute-value operator and $J(h_1, h_2, \cdots, h_L)$ is the Jacobian of the transformation, which is defined as

$$J(h_1, h_2, \cdots, h_L) = \begin{bmatrix} \frac{dr_1}{dh_1} & \cdots & \frac{dr_1}{dh_L} \\ \vdots & \ddots & \vdots \\ \frac{dr_L}{dh_1} & \cdots & \frac{dr_L}{dh_L} \end{bmatrix}. \tag{C.2}$$

In our case, $r_i = h_i^2$, $\frac{dr_i}{dh_j} = 2h_i$ when $i = j$; otherwise, $\frac{dr_i}{dh_j} = 0$. Therefore, $J(h_1, h_2, \cdots, h_L) = \prod_{i=1}^{L} 2h_i$. It is straightforward to obtain (2.25).